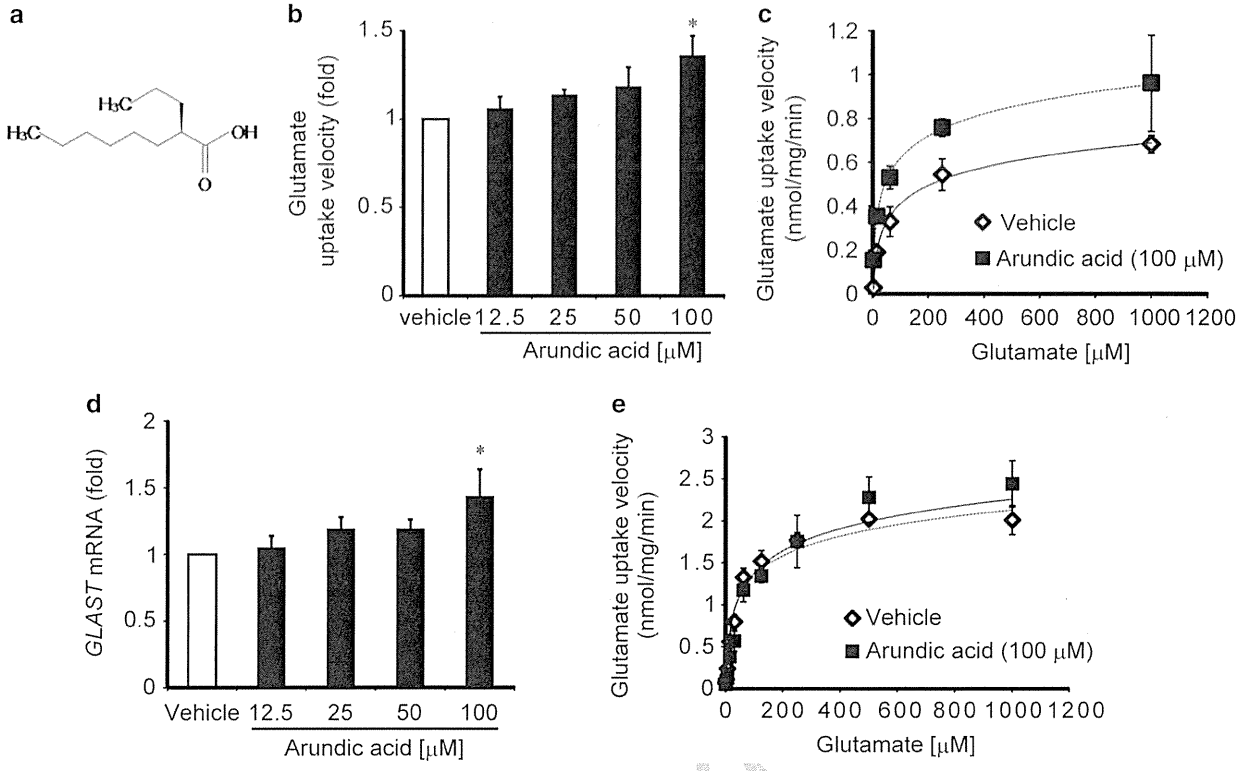

Figure 1 Arundic acid enhances glutamate uptake activity in Müller cells by an increase in the expression of *GLAST* mRNA. (**a**) Chemical structure of arundic acid. (**b**) In primary cultured Müller cells, glutamate transport is significantly increased after 14 days of treatment with 100 μM arundic acid. $^*P<0.05$ as determined by one-way ANOVA with Tukey–Kramer's *post hoc* analysis. (**c**) Representative transport kinetics saturation curves for L-[3,4-^{3}H]-glutamate uptake activity in primary cultured Müller cells treated with 100 μM arundic acid (closed square) or vehicle alone (open rhombus). Each data point corresponds to the mean ± S.E.M. of three individual determinations. (**d**) Effects of arundic acid on *GLAST* mRNA expression in primary cultured Müller cells. *GLAST* mRNA expression is significantly increased following 100 μM arundic acid treatment. $^*P<0.05$ as determined by one-way ANOVA with Dunnett's *post hoc* analysis. (**e**) Transport kinetics analysis of glutamate uptake activity by EAAT1-expressing HEK293T cells following treatment with 100 μM arundic acid (closed square) or vehicle alone (open rhombus). Data from three independent experiments generated mean values of 44.28 ± 9.22 μM for K_m and 2.04 ± 0.51 nmol/mg/min for V_{max}, in the absence of arundic acid, versus 54.96 ± 18.57 μM for K_m and 2.13 ± 0.53 nmol/mg/min for V_{max}, in the presence of arundic acid treatment. Thus, arundic acid had no effect on the kinetic properties of glutamate uptake by EAAT1-expressing HEK293T cells

to increase EAAT2 expression, few drugs increase the expression of EAAT1/GLAST.[16] Because of our specific interest in antiglaucoma therapies, we wish to identify drugs that elevate EAAT1/GLAST expression and activity.

Arundic acid ((2R)-2-propyloctanoic acid, ONO-2506; Figure 1a) was originally discovered through screening for an agent to inhibit synthesis of S100β in astrocytes.[17] A previous study showed that arundic acid administration markedly ameliorates brain damage in a transient middle cerebral artery occlusion rat model.[18] These beneficial effects of arundic acid are associated with marked suppression of delayed extracellular glutamate accumulation in the peri-infarct areas.[19] In searching for a possible mechanism of action, we hypothesized that arundic acid neuroprotection involves upregulation of EAAT1/GLAST.

To explore this hypothesis, we studied the effect of arundic acid on EAAT1/GLAST expression and glutamate uptake activity. These studies demonstrate that arundic acid can induce EAAT1/GLAST expression *in vitro* and *in vivo*. In addition, in GLAST heterozygous (*GLAST*$^{+/-}$) mice, treatment with arundic acid prevents RGC death, mediated through upregulation of GLAST.

Results

Arundic acid increases glutamate uptake in mouse Müller cells by increasing GLAST expression. To explore the postulated effects of arundic acid on glutamate uptake activity, first, we examined glutamate uptake in Müller cells that were prepared from retinas of C57BL/6 J mice and cultured for 14 days in the presence of 0–100 μM arundic acid. The glutamate uptake velocity was significantly increased by 100 μM arundic acid treatment (Figure 1b). Figure 1c shows the kinetic analysis of glutamate uptake in the presence and absence of 100 μM arundic acid. The V_{max} value of cells treated with arundic acid was 1.48 times that of cells treated with vehicle alone (Student's *t*-test, $P<0.05$), whereas the K_m value was not significantly affected (42.15 ± 18.98 μM for vehicle alone *versus* 30.52 ± 8.67 μM for arundic acid). These results suggest that arundic acid increases glutamate uptake activity by increasing V_{max}, without shifting the apparent glutamate affinity. One mechanism for increasing V_{max} is by increasing transporter expression. In Müller cells, GLAST is the most abundant glutamate transporter subtype.[20] Thus, we examined whether arundic acid increases *GLAST* expression in Müller cells by

quantitative real-time PCR (q RT-PCR). One hundred micromolar arundic acid significantly increased ($P<0.05$) endogenous *GLAST* mRNA expression in Müller cells (Figure 1d). The time course study reveled that arundic acid induced *GLAST* mRNA and protein expression as early as 24 h post-treatment (Supplementary Figures 1a and b). Because the transport process is driven by ion gradients, an arundic acid-mediated increase in glutamate uptake in Müller cells could be achieved indirectly by altering ion gradient across the plasma membrane. To explore this possibility, we examined the effect of arundic acid on glutamate uptake in HEK293T cells transfected with EAAT1 cDNA. In this system, arundic acid treatment did not alter the kinetic properties of EAAT1 (Figure 1e). Together, these results indicate that arundic acid treatment enhances glutamate uptake in Müller cells by increasing *GLAST* gene expression.

Arundic acid selectively enhances glutamate uptake via GLAST in the retina. To determine whether the effects of arundic acid are similar *in vivo*, we examined glutamate transporter expression in isolated mouse retinas treated with arundic acid. Three glutamate transporters are expressed around the synapses of RGCs in the plexiform layer, GLAST, GLT1 and excitatory amino-acid carrier 1 (EAAC1).[21] We administered arundic acid or vehicle to $GLAST^{+/-}$ mice during postnatal day (P) 22 to P35, and evaluated the glutamate transporter expression levels by qPCR. Arundic acid treatment increased *GLAST* mRNA expression in the retinas of $GLAST^{+/-}$ mice, but did not alter *GLT1* or *EAAC1* mRNA levels (Figure 2a). Next, we asked whether arundic acid is capable of increasing GLAST protein expression in the retinas of $GLAST^{+/-}$ mice. Using western blot analysis, we found that 14-day arundic acid treatment significantly

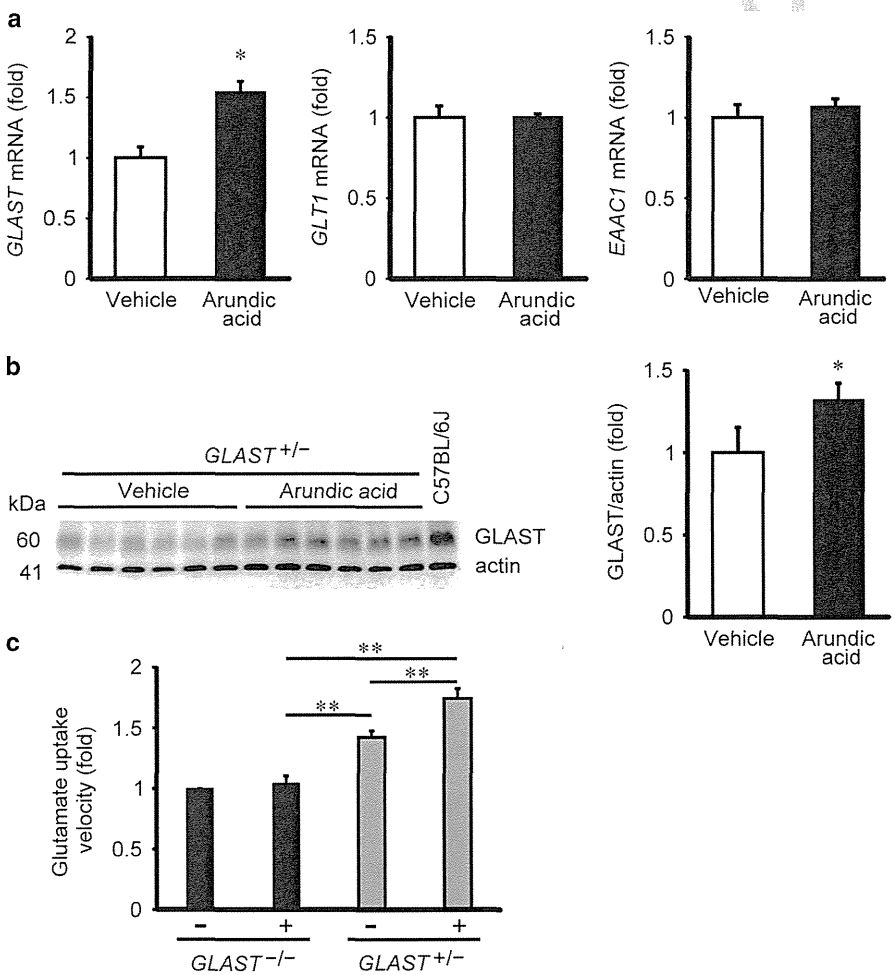

Figure 2 Arundic acid increases GLAST expression and transport activity in the mouse retina. (**a**) Effects of arundic acid treatment on *GLAST*, *GLT1* and *EAAC1* mRNA levels in the retina of $GLAST^{+/-}$ mice. Arundic acid (10 mg/kg, given daily from P22 to P35) increased the *GLAST* mRNA level ($N=6$), whereas the mRNA levels of *GLT1* ($N=6$) and *EAAC1* ($N=6$) are unaffected. $^*P<0.05$ as determined by a Student's *t*-test. (**b**) Arundic acid (10 mg/kg) increases GLAST protein expression in the retina of $GLAST^{+/-}$ mice relative to vehicle-treated control mice ($N=6$). A representative western blot of GLAST protein expression is shown; the quantified data represent the mean ± S.E.M. $^*P<0.05$ as determined by a Student's *t*-test. (**c**) Effect of arundic acid on glutamate uptake activity in the retina of GLAST mutant mice. Relative glutamate uptake velocity was quantified from six independent experiments performed in duplicate for each data point. Data represent the mean ± S.E.M. $^*P<0.05$, $^{**}P<0.01$ as determined by one-way ANOVA with Tukey–Kramer's *post hoc* analysis

increased endogenous GLAST protein expression (Figure 2b). To test whether the increases in GLAST mRNA and protein expression are accompanied by enhanced glutamate transport activity, we conducted L-[3,4-^{3}H]-glutamate uptake assays in isolated retinas from *GLAST*$^{+/-}$ and *GLAST*$^{-/-}$ mice. Fourteen-day arundic acid treatment led to a 1.23-fold increase in glutamate uptake in the retinas of *GLAST*$^{+/-}$ mice, compared with those treated with vehicle alone. We also observed that arundic acid increased GLAST protein expression and glutamate uptake activity in the retinas of wild-type mice (Supplementary Figures 2a and b). By contrast, arundic acid treatment did not affect glutamate uptake activity in the retinas of *GLAST*$^{-/-}$ mice (Figure 2c). These results suggest that arundic acid treatment increases retinal glutamate uptake activity by selectively increasing GLAST expression *in vivo*.

Arundic acid alleviates RGC loss by increasing GLAST expression in GLAST heterozygous mice. On the basis of the increased expression of GLAST described above, we hypothesized that arundic acid could be neuroprotective by protecting against RGC degeneration in GLAST-deficient mice. Chronic oral treatment of *GLAST*$^{+/-}$ mice with arundic acid, starting at 22 days of age, lead to a significant prevention of RGC loss compared with vehicle-treated control *GLAST*$^{+/-}$ mice (Figure 3). The number of cells in the ganglion cell layer (GCL) of *GLAST*$^{+/-}$ mice subjected to arundic acid treatment was significantly increased (438 ± 8 cells; $N=6$) relative to *GLAST*$^{+/-}$ mice without arundic acid treatment (366 ± 11 cells; $N=6$; Figures 3a and b). Neuroprotective effects of arundic acid cannot be seen with GLAST activation when studied in *GLAST*$^{-/-}$ mice. Taken together, these results suggested that arundic acid attenuates RGC loss in *GLAST*$^{+/-}$ mice by specifically facilitating GLAST expression.

Arundic acid facilitates the endogenous EAAT1 expression in human neuroglioblastoma cells via activating EAAT1 promoter. Although arundic acid can enhance the expression of GLAST in retina of mice, it remains unclear whether arundic acid increases the expression of endogenous *EAAT1* in human cells. To study the effect of arundic acid on endogenous *EAAT1* expression in human glial cells, H4 human neuroglioblastoma cells[22] were incubated with arundic acid for 9 days. *EAAT1* mRNA levels were quantified by qPCR. Treatment with 50 and 100 μM arundic acid significantly increased *EAAT1* mRNA expression in H4 cells (Figure 4a). To better understand the mechanism of action, we examined the effect of arundic acid on the promoter activity of *EAAT1* in H4 cells. Previous studies showed that the full-length human *EAAT1* promoter compromised the 2.3 kb region immediately flanking the 5′-end of the human *EAAT1* gene[22] and the 3′-UTR of the human *EAAT1* mediated the stimulatory influence of dbcAMP, epidermal growth factor, transforming growth factor α and pituitary adenylate cyclase-activating polypeptide on *EAAT1* expression.[23] Thus, H4 cells were transfected with a reporter plasmid containing the full-length human *EAAT1* promoter in combination with the 3′-UTR of the human *EAAT1* at 6 days after 50 μM arundic acid treatment. After 9 days of treatment of arundic acid, the cells were harvested and subjected to a luciferase reporter assay. Arundic acid significantly increased reporter gene activity of a construct containing the full-length human *EAAT1* promoter sequence as compared with vehicle-treated controls

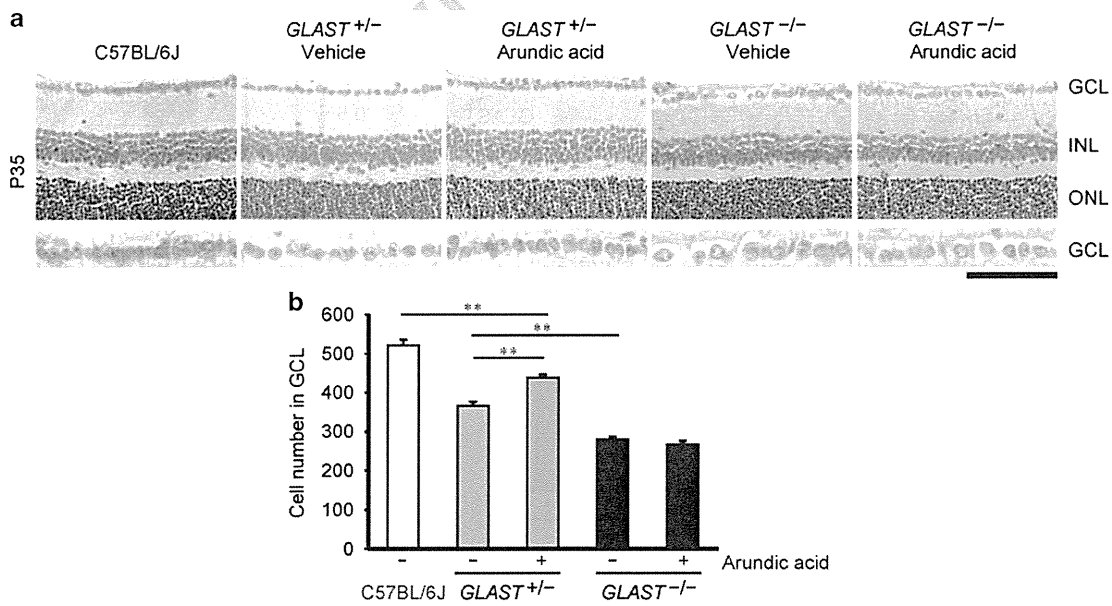

Figure 3 Arundic acid rescues RGC death in *GLAST*$^{+/-}$ mice by increasing GLAST expression. (**a**) Hematoxylin and eosin-stained retinal sections from wild-type, *GLAST*$^{+/-}$ and *GLAST*$^{-/-}$ mice at P35, with or without arundic acid (10 mg/kg) treatment. The scale bar represents 100 μm and 50 μm in the upper and lower panels, respectively. GCL, ganglion cell layer; INL, inner nuclear layer; ONL, outer nuclear layer. (**b**) Quantitative analyses of the number of neurons in the GCL following arundic acid treatment. The numbers of neurons in the GCL were counted in retinal sections from one ora serrata through the optic nerve to the other ora serrata ($N=6$). The data represent the mean ± S.E.M.. $^{**}P<0.01$ as determined by one-way ANOVA with Tukey–Kramer's *post hoc* analysis

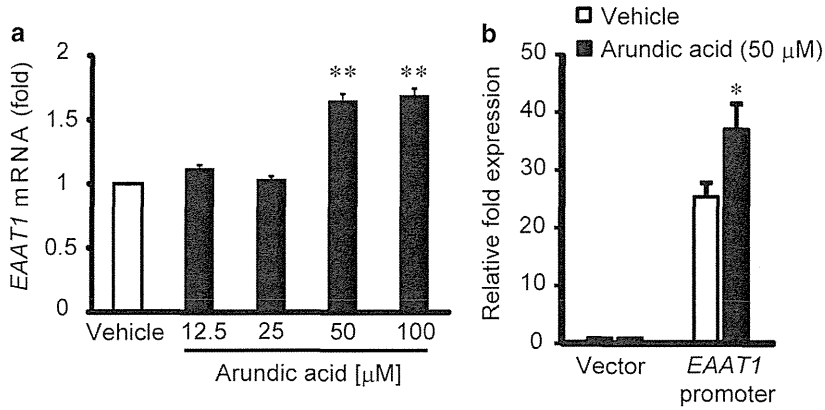

Figure 4 Arundic acid increases *EAAT1* mRNA and *EAAT1* promoter activity in human neuroglioblastoma H4 cells. (**a**) Arundic acid treatment resulted in an increase in *EAAT1* mRNA in the human H4 cell line, as evaluated by qPCR ($N=4$). Data represent the mean ± S.E.M. $^{**}P<0.01$ relative to control as determined by one-way ANOVA with Tukey–Kramer's *post hoc* analysis. (**b**) Arundic acid activates the *EAAT1* promoter. In human H4 cells transfected with the *EAAT1* promoter/luciferase reporter, 50 μM arundic acid significantly induced *EAAT1* promoter activity ($N=6$). Data represent the mean ± S.E.M. $^{*}P<0.05$ as determined by a Student's *t*-test

(Figure 4b). These data suggested that arundic acid can increase glutamate uptake in the human glial cells by activating the genetic promoter for *EAAT1*.

Discussion

Our previous study showed that GLAST-deficient mice develop NTG-like phenotypes,[5] which suggests that GLAST dysfunction may underlie or contribute to RGC loss in glaucoma patients. Importantly, deletion of *GLAST* in mice results in RGC degeneration without IOP elevation.[5] Currently, IOP reduction is the only proven treatment of glaucoma. However, it should be noted that some glaucoma patients are still progressive despite sufficient IOP reduction.[4] Thus, there is an urgent need for the discovery of alternative therapeutic approaches that are independent of IOP reduction and directed at preventing RGC loss. As glutamate excitotoxicity is involved in RGC loss in glaucoma,[9,10,24–26] drugs capable of increasing GLAST may be useful neuroprotective compounds. In recent years, a number of groups have identified clinically useful drugs that elevate EAAT2 levels.[13–15] However, there are few available drugs capable of increasing the expression of EAAT1/GLAST.[16] Various preclinical investigations have demonstrated the manifold beneficial actions of arundic acid against neurological diseases, including ischemic stroke,[27] Parkinson's disease,[28] amyotrophic lateral sclerosis[29] and Alzheimer's disease.[30] Although a lot of studies have assessed the inhibitory effect of arundic acid on the production and release of S100β protein from glial cells in these diseases, no study has examined the effect of arundic acid on the expression and activity of glutamate transporters. Because glutamate excitotoxicity is involved in these neurological diseases,[31] we hypothesized that the neuroprotective properties of arundic acid may, in part, involve the augmentation of EAAT1/GLAST. In this study, we demonstrated that arundic acid increases the EAAT/GLAST levels of the retina. This effect was specific to GLAST and did not alter the other subtypes of glutamate transporters, including the astroglial GLT1 and the neuronal EAAC1. It was reported that the neuroprotective action of arundic acid was mediated exclusively through the modulation of astrocytic function.[17] In the brain, GLAST and GLT1 are mainly localized in astrocytes.[32] However, in the retina, GLAST is expressed in Müller cells, whereas GLT1 is expressed only in a restricted set of neurons (mainly cone photoreceptors and cone bipolar cells).[20] Thus, the selective upregulation of GLAST in the retina by arundic acid can be explained by the selective localization of GLAST in Müller cells, the major type of glial cells in the retina.

A previous study suggested that GLAST is also important for maintaining glutathione levels in Müller cells by transporting glutamate into the cells.[5] Thus, GLAST dysfunction may lead to RGC degeneration through both excitotoxicity and oxidative stress. Arundic acid protected RGCs from oxidative and glutamate-induced injuries by increasing EAAT1/GLAST expression. Glutamate excitotoxicity and oxidative stress may contribute to retinal damage in various eye diseases, including retinal ischemia,[20] glaucoma,[33,34] diabetic retinopathy[35] and age-related macular degeneration.[36] In addition, if neurons that contain high concentrations of glutamate are injured, then there can also be secondary excitotoxic damage. Therefore, augmentation of EAAT1/GLAST activity with arundic acid treatment may be a novel strategy for the management of glaucoma and other various forms of retinopathy. Furthermore, we observed that arundic acid enhances the glutamate uptake activity and expression of glial glutamate transporters, GLT1 and GLAST, in the cerebral cortex of wild-type mice (Supplementary Figures 3a and b). Arundic acid may be useful for the treatment of other neuropsychiatric diseases, such as ataxia,[37,38] migraine,[39] schizophrenia[40–42] and depression[43] as glial glutamate transporter dysfunctions exist in these neuropsychiatric diseases. Arundic acid passed a phase 1 clinical trial,[27,44] so it does not cause toxicity in the central nervous system.

In addition, we demonstrated that arundic acid can enhance the EAAT1 expression in human neuroglioblastoma cells. The molecular mechanism of this enhancement appears to be activation of the genetic promoter for *EAAT1*, although the

pathway for promoter activation is not known. Our studies provide potential novel neurotherapeutics for the management of glaucoma by modulating the EAAT1 activity via gene activation.

Materials and Methods

Mice and arundic acid administration. All experiments were performed in accordance with the ethical guidelines of the Institutional Animal Care and Use Committee of Tokyo Medical and Dental University. C57BL/6 J mice were purchased from CLEA Japan (Tokyo, Japan). *GLAST*$^{+/-}$ and *GLAST*$^{-/-}$ mice were previously described.[45] All mice used in this study were backcrossed with C57BL/6 J mice for at least 10 generations. The daily oral administrations of arundic acid (10 mg/kg/day, Ono pharmaceutical)[30] or corn oil (Sigma-Aldrich, St. Louis, MO, USA) to C57BL/6 J, *GLAST*$^{+/-}$ and *GLAST*$^{-/-}$ mice were performed from ages P22 to P35. At a dose of 10 mg/kg, orally administered arundic acid was shown to exhibit inhibitory actions on cerebral amyloidosis and gliosis in Altzheimer transgenic mice.[30] The mice were killed immediately after the final administration and then their retinas were either processed for RGC counts, prepared for retinal RNA and protein extractions, or used for glutamate uptake assays.

Cell culture, transfection and luciferase assays. The primary Müller cell cultures were prepared as previously described.[6,46,47] The human neuroglioblastoma H4 cell line was purchased from American Type Tissue Collection (Manassas, VA, USA). Müller cells, H4 cells and HEK293T cells were grown in Dulbecco's modified Eagle's medium (Sigma-Aldrich) that contained 10% fetal bovine serum, 4.5 mg/ml D-glucose, 4 mM L-glutamine and 1 mM pyruvate at 37 °C in 10% CO_2/90% O_2. HEK293T cells were transfected with EAAT1 plasmid using GeneJuice Transfection Reagent (Merck Millipore, Billerica, MA, USA). One day after transfection, cells were plated onto 12-well plates at a density of 2.0×10^5 cells per well and incubated for 1 day. Two days after transfection, the cells were subjected to a glutamate uptake assay. To study the effects of arundic acid on EAAT1 expression in H4 cells, the cells were incubated for 9 days in culture media that contained arundic acid (0, 12.5, 25, 50 or 100 μM), and during which the media were changed every 2 days. To perform the luciferase promoter assay, after 6 days of 50 μM arundic acid or DMSO treatment, H4 cells were transiently transfected with the pGL4.11[*luc2P*] (Promega, Madison, WI, USA), containing the full-length promoter region and 3′-UTR of *EAAT1*, and pGL4.73[*hRluc/SV40*] (Promega), using Lipofectamine3000 (Invitrogen, Carlsbad, CA, USA). After transfection, the cells were incubated with 50 μM arundic acid or DMSO for three additional days. After 9 days of treatment, the cells were harvested with 1 x Passive Lysis Buffer (Promega). The luminescent signal from firefly luciferase and renilla luciferase was measured sequentially with a Lumat LB 9507 luminometer (Berthold Technologies, Bad Wildbad, Germany) using the Dual-Luciferase Reporter Assay System (Promega) according to the manufacturers' instructions. Firefly luciferase activity was normalized to renilla luciferase activity.

DNA constructs. Full-length EAAT1 cDNA (OriGene, Rockville, MD, USA) was cloned in the mammalian expression vector pcDNA3.1 (Invitrogen). Genomic DNA was extracted from H4 cells using a DNeasy Blood & Tissue Kit (Qiagen, Valencia, CA, USA), and the 2.7 kilobase (kb) fragment of the *EAAT1* promoter and 2.1 kb fragment of *EAAT1* 3′UTR were amplified by PCR. Primer sets were designed as follows: *EAAT1* promoter forward 5′-GCTCGCTAGCCTCGAGGTAATCTCGAGTT CTTCAAACCAAT-3′ and reverse 5′-CCGGATTGCCAAGCTTGGTGGAAGATAT CAAGCAGTAACG-3′; and *EAAT1* 3′-UTR forward 5′-AAATCGATAAGGATCCC GACAGTGAAACCAAGATGTAGAC-3′ and reverse 5′-AAGGGCATCGGTCTAC AAGAATAACAACAACGTGCAAAGA-3′. The PCR product of the EAAT1 promoter was inserted between the *Xho*I and *Hin*dIII sites of pGL4.11[*luc2P*] and cloned using an In-Fusion HD Cloning Kit (Clontech, Mountain View, CA, USA), and then the PCR product of *EAAT1* 3′UTR was similarly cloned following insertion between the *Bam*HI and *Sal*I sites of pGL4.11[*luc2P*].

Glutamate uptake assays. Two days after EAAT1 cDNA transfection, HEK293T cells were incubated at 37 °C for 12 min in assay buffer (137 mM NaCl, 5.4 mM KCl, 0.4 mM $MgSO_4$, 0.5 mM $MgCl_2$, 0.64 mM KH_2PO_4, 1.26 mM $CaCl_2$, 5 mM HEPES (pH 7.5) and 5.5 mM D(+)-glucose) containing 1.0, 3.9, 15.6, 62.5, 250.0 or 1000.0 μM of unlabeled L-glutamate. L-[3,4-^{3}H] glutamate (50.6 Ci/mmol, PerkinElmer Life Science, Boston, MA, USA) was added to a final concentration of 0.05 μM for an additional 20 min, following which the assay was terminated with two washes in ice-cold Na^+-free assay buffer (Na^+ was replaced by equimolar LiCl). Then the cells were immediately lysed with 0.1 N NaOH. Aliquots of the cell lysates were prepared for scintillation counting, whereas aliquots were used for the measurement of protein concentrations by a BCA kit (Sigma-Aldrich). The kinetic parameters, the Michaelis constant (K_m) and the maximum uptake velocity (V_{max}) were determined using Hanes–Woolf plot transformations. The effects of arundic acid on the kinetics of EAAT1 glutamate uptake activity were evaluated in cells following preincubation with arundic acid (100 μM) and subsequent addition of L-[3, 4-^{3}H] glutamate. In primary cultured Müller cells, the glutamate uptake assay was performed after 14 days of arundic acid treatment. Following 20 min of preincubation with assay buffer, glutamate uptake was terminated at 7 min by three washes in ice-cold Na^+-free assay buffer. All results were from triplicate samples and were repeated in three separate experiments. To determine the glutamate uptake velocity of retinas from C57BL/6 J- and GLAST-deficient mice, both retinas were removed from one mouse and cut into eight pieces. Each set of four pieces was preincubated with either Na^+-containing or Na^+-free assay buffer and 100 μM unlabeled glutamate for 20 min. L-[3,4-^{3}H] glutamate was added to a final concentration of 0.05 μM. After 7 min of incubation, the assay was terminated by washing three times with ice-cold Na^+-free assay buffer. The glutamate transport velocity was calculated by subtracting the velocity in Na^+-free assay buffer from that in Na^+-containing assay buffer. All results were performed in duplicate samples and were repeated in six individual mice.

Immunoblot analysis. Retinas and cultured Müller cells were homogenized in ice-cold 50 mM Tris-HCl (pH 7.5) containing 150 mM NaCl, 1% (v/v) Nonidet P-40, 0.25% (w/v) sodium deoxycholate, 1 mM EDTA, 1 mM phenylmethylsulfonyl fluoride, 1 mM $NaVO_4$, 1 mM NaF and a proteinase inhibitor cocktail (Roche, Manheim, Germany). Samples were separated by sodium dodecyl sulfate polyacrylamide gel electrophoresis and then transferred onto polyvinylidene difluoride membranes (Merck Millipore). The following antibodies were used for immunoblotting: 1 μg/ml of affinity purified anti-GLAST rabbit polyclonal[48] and 10 ng/mL of anti-β-actin mouse monoclonal (C4; Santa Cruz Biotechnology, Santa Cruz, CA, USA) antibodies. After incubation with primary antibodies, the membrane was incubated with horseradish peroxidase-conjugated mouse or rabbit immunoglobulin G antibodies (diluted 1 : 10 000; Jackson ImmunoResearch Laboratories, Bar Harbor, ME, USA). Data were visualized using Luminata Forte Western HRP Substrate (Merck Millipore) and quantified by measuring the ratio of band intensities for GLAST relative to β-actin using Image Lab software (Bio-Rad Laboratories, Hercules, CA, USA).

Quantitative RT-PCR experiments. Total mRNA was isolated from retinas and cells using TRIzol reagent (Invitrogen) and then reverse transcribed into cDNA using PrimeScript RT with gDNA Eraser (Takara Bio Inc. Siga, Japan). q RT-PCR was performed to amplify mouse *GLAST* (accession number: NM_148938.3), *GLT1* (accession number: NM_001077514.3), *EAAC1* (accession number: NM_009199.2) and *Rpp30* (the ortholog of human RNaseP, accession number: NM_019428.3). *EAAT1* and *RPPH1* (the H1 RNA subunit of the RNaseP enzyme complex, accession number: NR_002312.1) were amplified from human cells. The qPCR reactions were performed using a LightCycler 480 system II (Roche) with SYBR Premix ExTaq II (Takara Bio Inc.). The following primers were used: mouse *GLAST* forward 5′-GTCGCGGTGATAATGTGGTA-3′ and reverse 5′-AATCTTCCCTGC GATCAAGA-3′; mouse *GLT1* forward 5′-GGTCATCTTGGATGGAGGTC-3′ and reverse 5′-ATACTGGCTGCACCAATGC-3′; mouse *EAAC1* forward 5′-ACGT CACCCTGATCATTGCT-3′ and reverse 5′-GACGTTCACCATGGTCCTG-3′; mouse *Rpp30* forward 5′-TCCAGTGTGCAAGAAAGCTAAATG-3′ and reverse 5′-GGCA GTGCGTGGAGACTCA-3′; human *SLC1A3* forward 5′-TACCAAAGAGGAGGTT TGGC-3′ and reverse 5′-GGAGGGTCTCTTCTTTGCAC-3′; and human *RPPH1* forward 5′-AGCTGAGTGCGTCCTGTCACT-3′ and reverse 5′-TCTGGCCCTA GTCTCAGACCTT-3′. The qPCR experiments were conducted either three or four times, with every sample run in duplicate. The samples were normalized to the relative amplifications of mouse *Rpp30* and human *RPPH1*.

Histological and morphometric analysis. Mice were killed at P35 and then their eyes were dissected and immersed in Davidson's fixative solution[24] overnight at 4 °C. The fixed eyes were dehydrated in 70% ethanol for 3 days at 4 °C and embedded in paraffin wax. Embedded eyes were sectioned at a thickness of 7 μm and stained with hematoxylin and eosin. The number of neurons in the GCL was counted from one ora serrata through the optic nerve to the other ora serrata in a blind manner. The average numbers of neurons in the GCL/eyes were obtained

from three sections of each retina. Microscopic images were obtained using a Leica DM RA microscope (Leica, Wetzlar, Germany) with a HCX PLAN APO 40×/0.75 PH2 objective (Leica) and a DFC 300 FX camera (Leica), and a Leica Application Suite (Leica).

Statistical analyses. Values are expressed as the mean ± S.E.M. Two-tailed Student's *t*-tests were used for two-sample comparisons, and one-way ANOVA tests were used for multiple comparisons followed by Tukey–Kramer's or Dunnett's *post hoc* tests for significance, in which $P<0.05$ was regarded as statistically significant.

Conflict of Interest

The authors declare no conflict of interest.

Acknowledgements. This work was supported by the Strategic Research Program for Brain Sciences ('Understanding of molecular and environmental bases for brain health') from the Ministry of Education, Culture, Sports, Science and Technology of Japan (to KT), the Funding Program for Next Generation World-Leading Researchers (NEXT Program; to TH), a grant from the Ministry of Education, Culture, Sports, Science and Technology of Japan (to KN), a grant from the Ministry of Health, Labor and Welfare of Japan (to TH and KT), the Suzuken Memorial Foundation (to TA) and the Joint Usage/Research Program of the Medical Research Institute at Tokyo Medical and Dental University (to TH, TA and KT).

Author contributions

MY, TA, TH and KT designed the study. MY and KT wrote the paper. MY, RS, KN and TT conducted experiments. All authors interpreted the data.

1. Quigley HA, Broman AT. The number of people with glaucoma worldwide in 2010 and 2020. *Br J Ophthalmol* 2006; **90**: 262–267.
2. Weinreb RN, Khaw PT. Primary open-angle glaucoma. *Lancet* 2004; **363**: 1711–1720.
3. Iwase A, Suzuki Y, Araie M, Yamamoto T, Abe H, Shirato S *et al.* The prevalence of primary open-angle glaucoma in Japanese: the Tajimi Study. *Ophthalmology* 2004; **111**: 1641–1648.
4. Heijl A, Leske MC, Bengtsson B, Hyman L, Hussein M. Early Manifest Glaucoma Trial Group Reduction of intraocular pressure and glaucoma progression: results from the Early Manifest Glaucoma Trial. *Arch Ophthalmol* 2002; **120**: 1268–1279.
5. Harada T, Harada C, Nakamura K, Quah HM, Okumura A, Namekata K *et al.* The potential role of glutamate transporters in the pathogenesis of normal tension glaucoma. *J Clin Invest* 2007; **117**: 1763–1770.
6. Harada C, Namekata K, Guo X, Yoshida H, Mitamura Y, Matsumoto Y *et al.* ASK1 deficiency attenuates neural cell death in GLAST-deficient mice, a model of normal tension glaucoma. *Cell Death Differ* 2010; **17**: 1751–1759.
7. Izumi Y, Shimamoto K, Benz AM, Hammerman SB, Olney JW, Zorumski CF. Glutamate transporters and retinal excitotoxicity. *Glia* 2002; **39**: 58–68.
8. Reichelt W, Stabel-Burow J, Pannicke T, Weichert H, Heinemann U. The glutathione level of retinal Müller glial cells is dependent on the high-affinity sodium-dependent uptake of glutamate. *Neuroscience* 1997; **77**: 1213–1224.
9. Baltmr A, Duggan J, Nizari S, Salt TE, Cordeiro MF. Neuroprotection in glaucoma - is there a future role?. *Exp Eye Res* 2010; **91**: 554–566.
10. Naskar R, Vorwerk CK, Dreyer EB. Concurrent downregulation of a glutamate transporter and receptor in glaucoma. *Invest Ophthalmol Vis Sci* 2000; **41**: 1940–1944.
11. Namekata K, Harada C, Kohyama K, Matsumoto Y, Harada T. Interleukin-1 stimulates glutamate uptake in glial cells by accelerating membrane trafficking of Na+/K+-ATPase via actin depolymerization. *Mol Cell Biol* 2008; **28**: 3273–3280.
12. Koeberle PD, Bähr M. The upregulation of GLAST-1 is an indirect antiapoptotic mechanism of GDNF and neurturin in the adult CNS. *Cell Death Differ* 2008; **15**: 471–483.
13. Rothstein JD, Patel S, Regan MR, Haenggeli C, Huang YH, Bergles DE *et al.* Beta-lactam antibiotics offer neuroprotection by increasing glutamate transporter expression. *Nature* 2005; **433**: 73–77.
14. Tanaka K. Antibiotics rescue neurons from glutamate attack. *Trends Mol Med* 2005; **11**: 259–262.
15. Kong Q, Chang LC, Takahashi K, Liu Q, Schulte DA, Lai L *et al.* Small-molecule activator of glutamate transporter EAAT2 translation provides neuroprotection. *J Clin Invest* 2014; **124**: 1255–1267.
16. Fumagalli E, Funicello M, Rauen T, Gobbi M, Mennini T. Riluzole enhances the activity of glutamate transporters GLAST, GLT1 and EAAC1. *Eur J Pharmacol* 2008; **578**: 171–176.
17. Asano T, Mori T, Shimoda T, Shinagawa R, Satoh S, Yada N *et al.* Arundic acid (ONO-2506) ameliorates delayed ischemic brain damage by preventing astrocytic overproduction of S100B. *Curr Drug Targets CNS Neurol Disord* 2005; **4**: 127–142.
18. Tateishi N, Mori T, Kagamiishi Y, Satoh S, Katsube N, Morikawa E *et al.* Astrocytic activation and delayed infarct expansion after permanent focal ischemia in rats. Part II: suppression of astrocytic activation by a novel agent (R)-(-)-2-propyloctanoic acid (ONO-2506) leads to mitigation of delayed infarct expansion and early improvement of neurologic deficits. *J Cereb Blood Flow Metab* 2002; **22**: 723–734.
19. Mori T, Tateishi N, Kagamiishi Y, Shimoda T, Satoh S, Ono S *et al.* Attenuation of a delayed increase in the extracellular glutamate level in the peri-infarct area following focal cerebral ischemia by a novel agent ONO-2506. *Neurochem Int* 2004; **45**: 381–387.
20. Harada T, Harada C, Watanabe M, Inoue Y, Sakagawa T, Nakayama N *et al.* Functions of the two glutamate transporters GLAST and GLT-1 in the retina. *Proc Natl Acad Sci USA* 1998; **95**: 4663–4666.
21. Rauen T. Diversity of glutamate transporter expression and function in the mammalian retina. *Amino Acids* 2000; **19**: 53–62.
22. Kim SY, Choi SY, Chao W, Volsky DJ. Transcriptional regulation of human excitatory amino acid transporter 1 (EAAT1): cloning of the EAAT1 promoter and characterization of its basal and inducible activity in human astrocytes. *J Neurochem* 2003; **87**: 1485–1498.
23. Unger T, Lakowa N, Bette S, Engele J. Transcriptional regulation of the GLAST/EAAT-1 gene in rat and man. *Cell Mol Neurobiol* 2012; **32**: 539–547.
24. Bai N, Hayashi H, Aida T, Namekata K, Harada T, Mishina M *et al.* Dock3 interaction with a glutamate-receptor NR2D subunit protects neurons from excitotoxicity. *Mol Brain* 2013; **6**: 22.
25. Bai N, Aida T, Yanagisawa M, Katou S, Sakimura K, Mishina M *et al.* NMDA receptor subunits have different roles in NMDA-induced neurotoxicity in the retina. *Mol Brain* 2013; **6**: 34.
26. Namekata K, Kimura A, Kawamura K, Guo X, Harada C, Tanaka K *et al.* Dock3 attenuates neural cell death due to NMDA neurotoxicity and oxidative stress in a mouse model of normal tension glaucoma. *Cell Death Differ* 2013; **20**: 1250–1256.
27. Pettigrew LC, Kasner SE, Albers GW, Gorman M, Grotta JC, Sherman DG *et al.* Safety and tolerability of arundic acid in acute ischemic stroke. *J Neurol Sci* 2006; **251**: 50–56.
28. Oki C, Watanabe Y, Yokoyama H, Shimoda T, Kato H, Araki T. Delayed treatment with arundic acid reduces the MPTP-induced neurotoxicity in mice. *Cell Mol Neurobiol* 2008; **28**: 417–430.
29. Traynor BJ, Bruijn L, Conwit R, Beal F, O'Neill G, Fagan SC *et al.* Neuroprotective agents for clinical trials in ALS: a systematic assessment. *Neurology* 2006; **67**: 20–27.
30. Mori T, Town T, Tan J, Yada N, Horikoshi Y, Yamamoto J *et al.* Arundic Acid ameliorates cerebral amyloidosis and gliosis in Alzheimer transgenic mice. *J Pharmacol Exp Ther* 2006; **318**: 571–578.
31. Mehta A, Prabhakar M, Kumar P, Deshmukh R, Sharma PL. Excitotoxicity: bridge to various triggers in neurodegenerative disorders. *Eur J Pharmacol* 2013; **698**: 6–18.
32. Takasaki C, Okada R, Mitani A, Fukaya M, Yamasaki M, Fujihara Y *et al.* Glutamate transporters regulate lesion-induced plasticity in the developing somatosensory cortex. *J Neurosci* 2008; **28**: 4995–5006.
33. Martin KR, Levkovitch-Verbin H, Valenta D, Baumrind L, Pease ME, Quigley HA. Retinal glutamate transporter changes in experimental glaucoma and after optic nerve transection in the rat. *Invest Ophthalmol Vis Sci* 2002; **43**: 2236–2243.
34. Schuettauf F, Thaler S, Bolz S, Fries J, Kalbacher H, Mankowska A *et al.* Alterations of amino acids and glutamate transport in the DBA/2J mouse retina; possible clues to degeneration. *Graefes Arch Clin Exp Ophthalmol* 2007; **245**: 1157–1168.
35. Li Q, Puro DG. Diabetes-induced dysfunction of the glutamate transporter in retinal Müller cells. *Invest Ophthalmol Vis Sci* 2002; **43**: 3109–3116.
36. Kinnunen K, Petrovski G, Moe MC, Berta A, Kaarniranta K. Molecular mechanisms of retinal pigment epithelium damage and development of age-related macular degeneration. *Acta Ophthalmol* 2012; **90**: 299–309.
37. Jen JC, Wan J, Palos TP, Howard BD, Baloh RW. Mutation in the glutamate transporter EAAT1 causes episodic ataxia, hemiplegia, and seizures. *Neurology* 2005; **65**: 529–534.
38. de Vries B, Mamsa H, Stam AH, Wan J, Bakker SL, Vanmolkot KR *et al.* Episodic ataxia associated with EAAT1 mutation C186S affecting glutamate reuptake. *Arch Neurol* 2009; **66**: 97–101.
39. Freilinger T, Koch J, Dichgans M, Mamsa H, Jen J. A novel mutations in SLC1A3 associated with pure hemiplegic migraine. *J Headache Pain* 2010. Q4
40. Walsh T, McClellan JM, McCarthy SE, Addington AM, Pierce SB, Cooper GM *et al.* Rare structural variants disrupt multiple genes in neurodevelopmental pathways in schizophrenia. *Science* 2008; **320**: 539–543.
41. Karlsson RM, Tanaka K, Heilig M, Holmes A. Loss of glial glutamate and aspartate transporter (excitatory amino acid transporter 1) causes locomotor hyperactivity and exaggerated responses to psychotomimetics: rescue by haloperidol and metabotropic glutamate 2/3 agonist. *Biol Psychiatry* 2008; **64**: 810–814.
42. Karlsson RM, Tanaka K, Saksida LM, Bussey TJ, Heilig M, Holmes A. Assessment of glutamate transporter GLAST (EAAT1)-deficient mice for phenotypes relevant to the

negative and executive/cognitive symptoms of schizophrenia. *Neuropsychopharmacology* 2009; **34**: 1578–1589.
43. Cui W, Mizukami H, Yanagisawa M, Aida T, Nomura M, Isomura Y *et al.* Glial dysfunction in the mouse habenula causes depressive-like behaviors and sleep disturbance. *J Neurosci* 2014; **34**: 16273–16285.
44. Ishibashi H, Pettigrew LC, Funakoshi Y, Hiramatsu M. Pharmacokinetics of arundic acid, an astrocyte modulating agent, in acute ischemic stroke. *J Clin Pharmacol* 2007; **47**: 445–452.
45. Watase K, Hashimoto K, Kano M, Yamada K, Watanabe M, Inoue Y *et al.* Motor discoordination and increased susceptibility to cerebellar injury in GLAST mutant mice. *Eur J Neurosci* 1998; **10**: 976–988.
46. Harada T, Harada C, Kohsaka S, Wada E, Yoshida K, Ohno S *et al.* Microglia-Müller glia cell interactions control neurotrophic factor production during light-induced retinal degeneration. *J Neurosci* 2002; **22**: 9228–9236.
47. Harada C, Harada T, Quah HM, Maekawa F, Yoshida K, Ohno S *et al.* Potential role of glial cell line-derived neurotrophic factor receptors in Müller glial cells during light-induced retinal degeneration. *Neuroscience* 2003; **122**: 229–235.
48. Shibata T, Yamada K, Watanabe M, Ikenaka K, Wada K, Tanaka K *et al.* Glutamate transporter GLAST is expressed in the radial glia-astrocyte lineage of developing mouse spinal cord. *J Neurosci* 1997; **17**: 9212–9219.

Supplementary Information accompanies this paper on Cell Death and Disease website (http://www.nature.com/cddis)

Neuroscience Letters 588 (2015) 108–113

Contents lists available at ScienceDirect

Neuroscience Letters

journal homepage: www.elsevier.com/locate/neulet

Research article

Valproic acid prevents retinal degeneration in a murine model of normal tension glaucoma

Atsuko Kimura[a], Xiaoli Guo[a], Takahiko Noro[a], Chikako Harada[a], Kohichi Tanaka[b], Kazuhiko Namekata[a], Takayuki Harada[a,*]

[a] Visual Research Project, Tokyo Metropolitan Institute of Medical Science, Tokyo, Japan
[b] Laboratory of Molecular Neuroscience, Medical Research Institute, Tokyo Medical and Dental University, Tokyo, Japan

HIGHLIGHTS

- The concept that VPA exerts neuroprotective effects is emerging.
- We examine the therapeutic potential of VPA in a mouse model of normal tension glaucoma.
- VPA suppresses glaucomatous retinal degeneration in GLAST KO mice.
- VPA ameliorates visual impairment in GLAST KO mice.
- VPA may be useful for preventing retinal ganglion cell death and preserving sight in glaucoma patients.

ARTICLE INFO

Article history:
Received 30 November 2014
Received in revised form
22 December 2014
Accepted 25 December 2014
Available online 30 December 2014

Keywords:
Valproic acid
Normal tension glaucoma
GLAST KO mice
Neuroprotection
Oxidative stress
ERK

ABSTRACT

Valproic acid (VPA) is widely used for treatment of epilepsy, mood disorders, migraines and neuropathic pain. It exerts its therapeutic benefits through modulation of multiple mechanisms including regulation of gamma-aminobutyric acid and glutamate neurotransmissions, activation of pro-survival protein kinases and inhibition of histone deacetylase. The evidence for neuroprotective properties associated with VPA is emerging. Herein, we investigated the therapeutic potential of VPA in a mouse model of normal tension glaucoma (NTG). Mice with glutamate/aspartate transporter gene deletion (GLAST KO mice) demonstrate progressive retinal ganglion cell (RGC) loss and optic nerve degeneration without elevated intraocular pressure, and exhibit glaucomatous pathology including glutamate neurotoxicity and oxidative stress in the retina. VPA (300 mg/kg) or vehicle (PBS) was administered via intraperitoneal injection in GLAST KO mice daily for 2 weeks from the age of 3 weeks, which coincides with the onset of glaucomatous retinal degeneration. Following completion of the treatment period, the vehicle-treated GLAST KO mouse retina showed significant RGC death. Meanwhile, VPA treatment prevented RGC death and thinning of the inner retinal layer in GLAST KO mice. In addition, in vivo electrophysiological analyses demonstrated that visual impairment observed in vehicle-treated GLAST KO mice was ameliorated with VPA treatment, clearly establishing that VPA beneficially affects both histological and functional aspects of the glaucomatous retina. We found that VPA reduces oxidative stress induced in the GLAST KO retina and stimulates the cell survival signalling pathway associated with extracellular-signal-regulated kinases (ERK). This is the first study to report the neuroprotective effects of VPA in an animal model of NTG. Our findings raise intriguing possibilities that the widely prescribed drug VPA may be a novel candidate for treatment of glaucoma.

Abbreviations: 2K, second order kernel; 4-HNE, 4-hydroxy-2-nonenal; BDNF, brain-derived neurotrophic factor; ERK, extracellular-signal-regulated kinases; GCL, ganglion cell layer; GLAST, glutamate/aspartate transporter; HDAC, histone deacetylase; INL, inner nuclear layer; IOP, intraocular pressure; IRL, inner retinal layer; mfERG, multifocal electroretinogram; NMDA, *N*-methyl-D-aspartate; NTG, normal tension glaucoma; ONL, outer nuclear layer; RGC, retinal ganglion cell; VPA, valproic acid.

* Corresponding author at: Visual Research Project, Tokyo Metropolitan Institute of Medical Science, 2-1-6 Kamikitazawa, Setagaya-ku, Tokyo 156-8506, Japan. Tel.: +81 3 6834 2338; fax: +81 3 6834 2339.
E-mail address: harada-tk@igakuken.or.jp (T. Harada).

http://dx.doi.org/10.1016/j.neulet.2014.12.054
0304-3940/

1. Introduction

Glaucoma is one of the major causes of blindness in the world. It is estimated that glaucoma will affect more than 80 million individuals worldwide by 2020, with at least 6–8 million individuals becoming bilaterally blind [31]. Glaucoma is characterized by progressive loss of retinal ganglion cells (RGCs) and their axons that comprise the optic nerve, which are usually associated with elevated intraocular pressure (IOP), but there is also a subtype of glaucoma termed normal tension glaucoma (NTG) that presents with statistically normal IOP. The general concept is that the number of NTG patients is small relative to the total number of glaucoma patients, but there is an unexpectedly high prevalence of NTG in Japan [18]. Previously, we developed two mouse models of NTG by deleting the glutamate transporter genes glutamate/aspartate transporter (GLAST) and excitatory amino-acid carrier 1 (EAAC1) [16]. GLAST and EAAC1 knockout (KO) mice show progressive RGC loss and optic nerve degeneration without elevated IOP, and exhibit glaucomatous pathology including glutamate neurotoxicity and oxidative stress in the retina. These animal models have been extremely useful in providing information on therapeutic target for NTG [15,25,27,28,33,34].

Valproic acid (VPA) is a short-chain fatty acid and is used worldwide clinically for treatment of epilepsy, mood disorders, migraines and neuropathic pain [7,17,21,37]. The pharmacological action of VPA involves multiple mechanisms including those associated with modulation of glutamate and gamma-aminobutyric acid (GABA) neurotransmissions, and those that affects intracellular signal transduction pathways; more specifically, by modulating enzymatic activities, such as extracellular-signal-regulated kinases (ERK), phosphatidylinositol 3-kinase/Akt-1, and glycogen synthase kinase 3β, as well as histone deacetylase (HDAC) [4,8,10,11,30,39]. Recently, the concept that VPA exerts neuroprotective effects has emerged [5,24]. In this study, we investigated the therapeutic potential of VPA in glaucomatous retinal degeneration presented by a mouse model of NTG.

2. Materials and methods

2.1. Animals

Experiments were performed using C57 BL/6J mice (WT; CLEA Japan, Tokyo, Japan) and GLAST KO mice [16] in accordance with the Tokyo Metropolitan Institute of Medical Science Guidelines for the Care and Use of Animals.

2.2. Drug treatment

WT and GLAST KO mice at 3 weeks old of age received daily intraperitoneal administration of vehicle (PBS) or VPA (300 mg/kg) for 2 weeks.

2.3. Histological analyses

At the end of the experimental period, mice were perfused with Zamboni's Fixative (2% paraformaldehyde and 15% picric acid in 0.1 M phosphate buffer). Eyes were enucleated and post-fixed in 3% glutaraldehyde solution (3% glutaraldehyde, 9% formaldehyde, 37.5% ethanol and 12.5% acetic acid in distilled water) for 2 h. Paraffin embedded retinal sections of 7 μm thickness were cut through the optic nerve and stained with haematoxylin and eosin (H&E). The extent of retinal degeneration was quantified as previously reported [14].

2.4. Multifocal electroretinogram (mfERG)

Mice were anaesthetized by intraperitoneal injection of sodium pentobarbital (87.5 mg/kg). The pupils were dilated with 0.5% phenylephrine hydrochloride and 0.5% tropicamide. mfERGs were recorded using a VERIS 6.0 system (Electro-Diagnostic Imaging, Redwood City, CA, USA). The visual stimulus consisted of seven hexagonal areas scaled with eccentricity. The stimulus array was displayed on a high-resolution black and white monitor driven at a frame rate of 100 Hz. The second-order kernel (2K), which is impaired in patients with glaucoma, was analysed [16].

2.5. Immunohistochemistry

Following completion of the treatment period, GLAST KO mice were perfused with Zamboni's Fixative. Eyes were enucleated, postfixed in Zamboni's Fixative for 1 h and then transferred into a sucrose buffer (30% sucrose in a 0.1 M phosphate buffer) for cryoprotection. Retinal cryostat sections of 10 μm thickness were prepared and examined by immunostaining as previously reported [14], using a 4-hydroxy-2-nonenal (4-HNE) mouse monoclonal antibody (2 μg/ml; Japan Institute for the Control of Aging, Shizuoka, Japan). The intensity of 4-HNE at the ganglion cell layer (GCL) was analysed using ImageJ (NIH, Bethesda, MD, USA).

2.6. Immunoblot analyses

Mice were anaesthetized by intraperitoneal injection of sodium pentobarbital (87.5 mg/kg) and received intravitreal injections of vehicle or VPA (2 μl; 75 mM) [20]. Mice were killed by cervical dislocation 1 h after the injection and retinas were isolated in ice-cold PBS. Immunoblotting was carried out as previously described [14,26] and the expression of ERK was detected using antibodies against total ERK and phosphorylated ERK (1:1000; BD biosciences, San Diego, CA, USA).

2.7. Statistics

For statistical comparison of two samples, we used a two-tailed Student's *t*-test. Data are presented as means ± S.E.M. $P < 0.05$ was regarded as statistically significant.

3. Results

3.1. VPA suppresses loss of RGCs in GLAST KO mice

In order to examine the effects of VPA on glaucomatous pathology, we first examined histopathology of the GLAST KO mouse retina with or without VPA treatment. The cell number in the GCL of vehicle-treated GLAST KO mice was significantly declined compared with the vehicle-treated WT mice, which is consistent with the previous reports [15,16,27], while VPA-treatment in GLAST KO mice reduced the extent of this damage (Fig. 1A and B). In addition, thinning of the inner retinal layer [IRL; between the internal limiting membrane and the interface of the outer plexiform layer and the outer nuclear layer (ONL)] in vehicle-treated GLAST KO mice was suppressed in VPA-treated GLAST KO mice (Fig. 1C). VPA treatment had no effects on the WT mouse retina (data not shown). These results demonstrate that daily VPA treatment suppresses glaucomatous retinal degeneration in GLAST KO mice.

3.2. VPA ameliorates visual impairment in GLAST KO mice

In order to determine if the histological observation of VPA-mediated neuroprotection in GLAST KO mice reflects functional aspects, we examined visual function using mfERG. We analysed

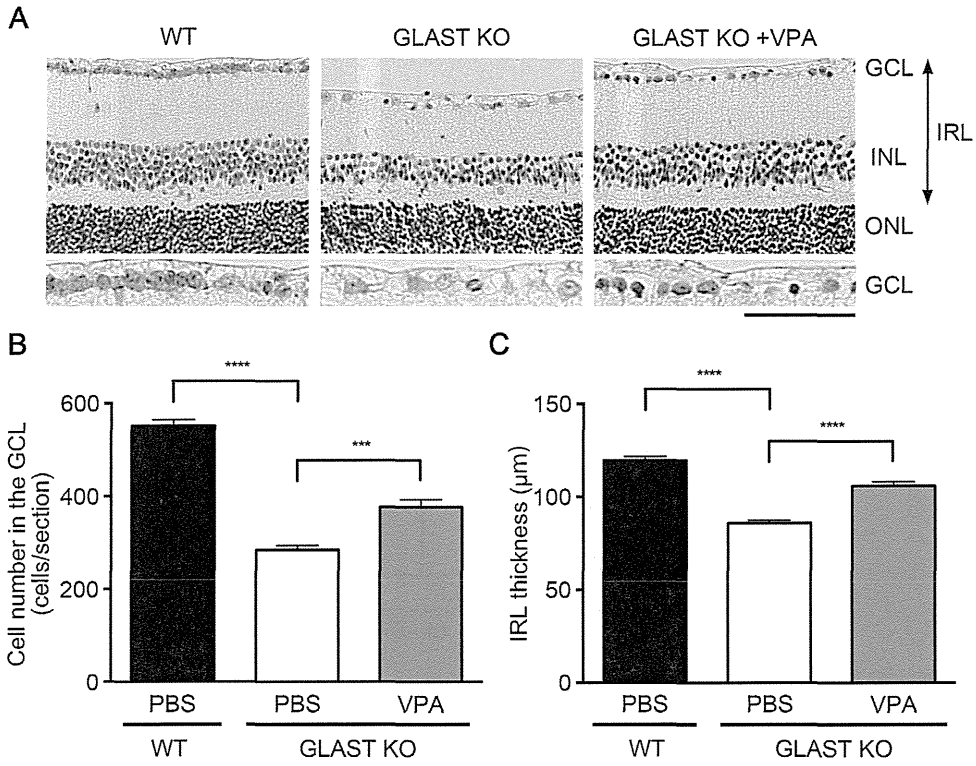

Fig. 1. VPA suppresses loss of RGCs in GLAST KO mice.
(A) H&E staining of representative retinal sections from vehicle-treated wild-type mice (WT) and vehicle- or VPA (300 mg/kg, i.p.)-treated GLAST KO mice (GLAST KO and GLAST KO + VPA, respectively) after 2 weeks of treatment. Scale bar: 100 and 50 μm for the upper and immediately lower panels, respectively. GCL, ganglion cell layer; INL, inner nuclear layer; ONL, outer nuclear layer; IRL, inner retinal layer. (B, C) Quantitative analyses of (A): cell number in the GCL per section (B); and IRL thickness (C). Data are presented as means ± S.E.M., $n = 6$. $^{***}P < 0.001$; $^{****}P < 0.0001$.

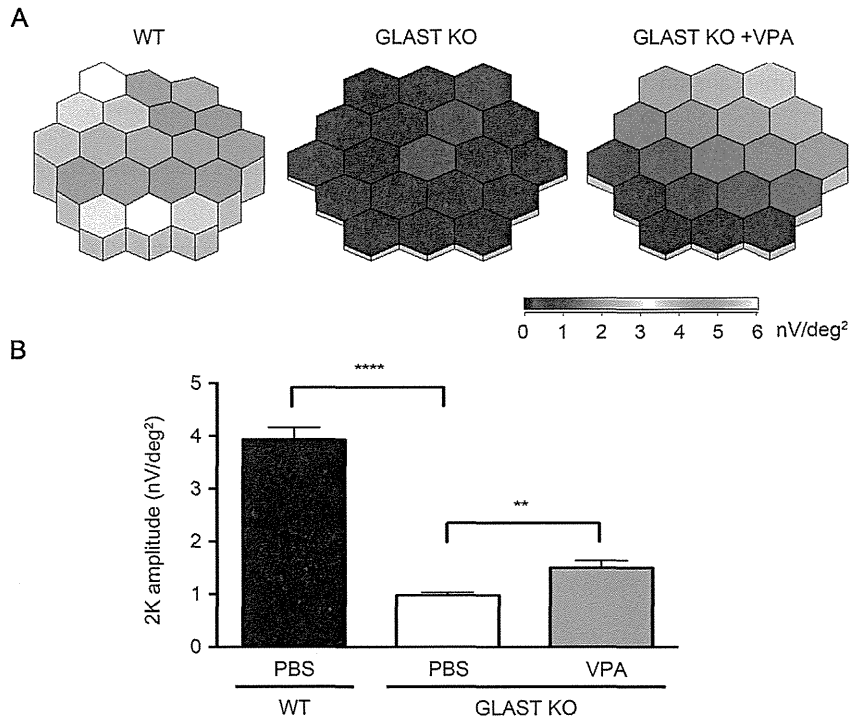

Fig. 2. VPA ameliorates visual impairment in GLAST KO mice. (For interpretation of the references to colour in this figure legend, the reader is referred to the web version of this article.)
(A) Representative images of three-dimensional plots depicting averaged visual responses of the second-order kernel (2K) examined by mfERG, in vehicle-treated WT mice and vehicle- or VPA (300 mg/kg, i.p.)-treated GLAST KO mice after 2 weeks of treatment. The degree of retinal function is presented in the colour bar. A higher score (red) indicates highly sensitive visual function, and a lower score (green) indicates retinal dysfunction. (B) Quantitative analysis of (A). Values are expressed in nV per square degree (nV/deg^2). Data are presented as means ± S.E.M., $n = 6$. $^{**}P < 0.01$; $^{****}P < 0.0001$.

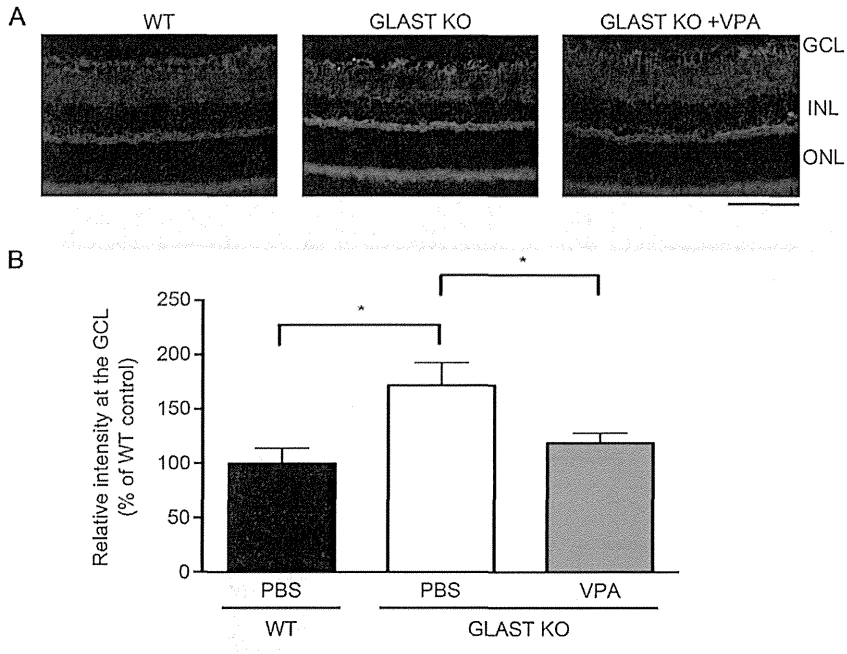

Fig. 3. VPA reduces the oxidative stress level in the GLAST KO mouse retina.
(A) Representative images of the 4-HNE expression in the retina of vehicle-treated WT mice and vehicle- or VPA (300 mg/kg, i.p.)-treated GLAST KO mice after 2 weeks of treatment. Scale bar: 100 μm. (B) Quantitative analyses of (A). Data are normalized to the 4-HNE intensity at the GCL in vehicle-treated WT mice (100%). Data are presented as means ± S.E.M., $n = 4$. $^{*}P < 0.05$.

the 2K component, which appears to be a sensitive indicator of inner retinal dysfunction and is impaired in glaucoma patients [2]. The response topography demonstrating the 2K component revealed that the average visual responses were impaired in all visual fields in GLAST KO mice, but VPA treatment ameliorated the deterioration in visual function (Fig. 2A and B). VPA treatment had no effects on the WT mouse retina (data not shown). These results verify that the neuroprotective effects of VPA on glaucomatous retinal degeneration in GLAST KO mice are functionally significant.

3.3. VPA reduces the oxidative stress level in the GLAST KO mouse retina

We next investigated potential mechanisms underlying VPA-mediated neuroprotection. One of the major causes that is associated with glaucomatous retinal degeneration in GLAST KO mice is increased oxidative stress levels [16]. Therefore, we examined if VPA treatment suppresses induction of oxidative stress in GLAST KO mice. The expression of 4-HNE, which provides a reliable measure of oxidative stress [22], was detected in the RGCs of vehicle-treated GLAST KO mice, but it was hardly detected in the RGCs of vehicle-treated WT mice or VPA-treated GLAST KO mice (Fig. 3A). Quantitative analyses confirmed that the oxidative stress level in the GCL is significantly suppressed with VPA treatment in GLAST KO mice (Fig. 3B). VPA treatment had no effects on the WT mouse retina (data not shown).

3.4. VPA stimulates cell survival signalling in the GLAST KO mouse retina

We also investigated if VPA has any effects on stimulation of cell survival signalling pathways in the GLAST KO mouse retina.

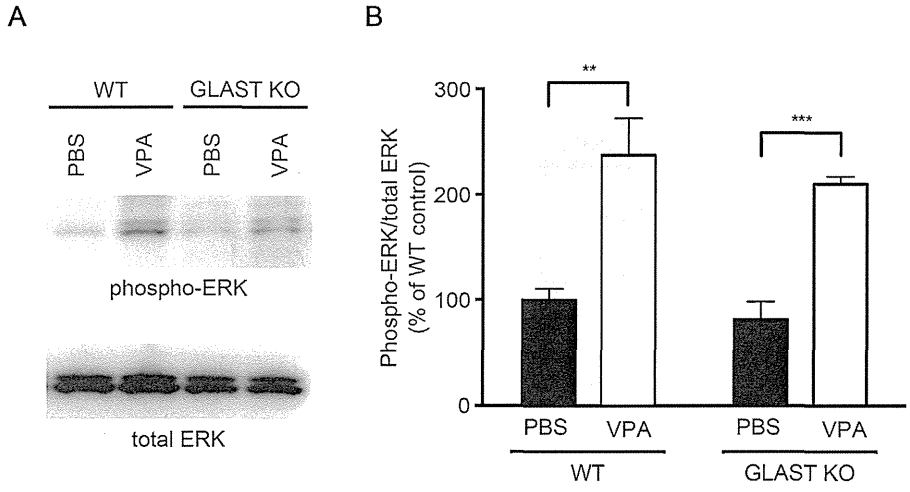

Fig. 4. VPA increases ERK phosphorylation in the GLAST KO mouse retina.
(A) Representative images of immunoblot analyses of total and phosphorylated ERK in WT or GLAST KO retinas with intravitreal injection of vehicle or VPA. (B) Quantitative analyses of (A). Data are normalized to the phospho-ERK/total ERK ratio in vehicle-treated WT mice (100%). Data are presented as means ± S.E.M., $n = 4$. $^{**}P < 0.01$; $^{***}P < 0.001$.

Previously, it was reported that activation of the ERK signalling pathway leads to RGC protection in glaucomatous eyes [44] and therefore, we examined the level of ERK phosphorylation. VPA increases phosphorylation of ERK in the GLAST KO mouse retina, as well as in the WT mouse retina (Fig. 4), indicating that activation of ERK-mediated cell survival signalling is one of the neuroprotective mechanisms associated with VPA treatment in GLAST KO mice.

4. Discussion

Herein, we demonstrate that VPA prevents glaucomatous retinal degeneration in GLAST KO mice. This is the first study to report neuroprotective effects of VPA on an animal model of NTG. We show that VPA treatment prevented RGC death in GLAST KO mice and substantiate these histological observations with physiological significance by employing an effective non-invasive method to measure visual function in living animals. We also show that VPA treatment reduces oxidative stress levels in RGCs of GLAST KO mice and that it stimulates phosphorylation of ERK in the GLAST KO mouse retina. These findings indicate that VPA exerts neuroprotective effects through suppression of oxidative stress and stimulation of cell survival signalling in GLAST KO mice.

Oxidative stress is an important risk factor in human glaucoma [9] and suppression of oxidative stress in RGCs is a potential treatment strategy for glaucoma [28,29]. In this study, we demonstrate that VPA suppresses the oxidative stress levels in the glaucomatous retina. Consistently, we previously showed that VPA exerts neuroprotective effects by reducing oxidative stress levels in the RGCs of an NMDA-excitotoxicity model [20] and other studies have shown anti-oxidant properties of VPA in the brain and retina of stroke models [36,41,42]. These findings support our conclusion that one of the VPA-mediated neuroprotective mechanisms in the GLAST KO mouse retina is suppression of oxidative stress.

The ERK signalling pathway is one of the key regulatory intracellular signalling pathways for cell proliferation and survival [32]. Activation of this pathway mediates pro-survival effects on axotomized RGCs [6,19] and on RGCs in experimental ocular hypertension model [44]. In this study, we show that VPA increases ERK phosphorylation in the glaucomatous eye. VPA has been reported to exert neuroprotective effects by stimulating the ERK pathway in cortical neurons [11] and in the retina following optic nerve injury [4,43]. VPA stimulates ERK phosphorylation through a mechanism that is independent of HDAC inhibition, and suppresses apoptosis [23], suggesting that VPA may exert a direct effect on ERK activation. These observations suggest a vital role of the ERK pathway in VPA-mediated neuroprotection.

It is important to note the possibility that other pathways are also involved in VPA-mediated neuroprotection. For example, we previously reported that VPA upregulates Müller glial brain-derived neurotrophic factor (BDNF) and nerve growth factor, neurotrophic factors important for cell survival [12,13,20] and these effects may also apply to the VPA-treated GLAST KO mouse retina. Also, VPA is an effective HDAC inhibitor [8,30] and increased histone acetylation is associated with VPA-mediated neuroprotection [1,3,35,40,43]. These findings urge to identify genes and pathways that are modulated by HDAC inhibition and are involved in VPA-mediated RGC protection. Furthermore, VPA reduces glutamatergic excitatory neurotransmission by suppressing NMDA-evoked depolarisation [38], suggesting that excitotoxic damage in GLAST KO mice may be decreased by VPA treatment.

In conclusion, we report that the widely prescribed drug VPA exerts neuroprotective effects on retinal degeneration in a mouse model of NTG. Our findings raise an interesting possibility that VPA may be a novel candidate for treatment of glaucoma.

Conflict of interest

All authors declare that they have no conflicts of interest.

Acknowledgments

We would like to thank M. Kunitomo, K. Okabe and Y. Azuchi for their technical assistance. This study was supported by the Ministry of Education, Culture, Sports, Science and Technology of Japan (AK, XG, CH, KN, TH), and the Funding Program for Next Generation World-Leading Researchers (NEXT Program) (TH).

References

[1] O. Alsarraf, J. Fan, M. Dahrouj, C.J. Chou, P.W. Yates, C.E. Crosson, Acetylation preserves retinal ganglion cell structure and function in a chronic model of ocular hypertension, Invest. Ophthalmol. Visual Sci. 55 (2014) 7486–7493.
[2] M.A. Bearse, E.E. Sutter Jr., D. Sim, R. Stamper, Glaucomatous dysfunction revealed in higher order components of the electroretinogram, Vision Sci. Appl. 1 (1996) 105–107.
[3] J. Biermann, J. Boyle, A. Pielen, W.A. Lagreze, Histone deacetylase inhibitors sodium butyrate and valproic acid delay spontaneous cell death in purified rat retinal ganglion cells, Mol. Vision 17 (2011) 395–403.
[4] J. Biermann, P. Grieshaber, U. Goebel, G. Martin, S. Thanos, S. Di Giovanni, W.A. Lagreze, Valproic acid-mediated neuroprotection and regeneration in injured retinal ganglion cells, Invest. Ophthalmol. Visual Sci. 51 (2010) 526–534.
[5] S. Chen, H. Wu, D. Klebe, Y. Hong, J. Zhang, Valproic Acid: a new candidate of therapeutic application for the acute central nervous system injuries, Neurochem. Res. 39 (2014) 1621–1633.
[6] L. Cheng, P. Sapieha, P. Kittlerova, W.W. Hauswirth, A. Di Polo, TrkB gene transfer protects retinal ganglion cells from axotomy-induced death in vivo, J. Neurosci. 22 (2002) 3977–3986.
[7] C.T. Chiu, Z. Wang, J.G. Hunsberger, D.M. Chuang, Therapeutic potential of mood stabilizers lithium and valproic acid: beyond bipolar disorder, Pharmacol. Rev. 65 (2013) 105–142.
[8] M. Gottlicher, S. Minucci, P. Zhu, O.H. Kramer, A. Schimpf, S. Giavara, J.P. Sleeman, F. Lo Coco, C. Nervi, P.G. Pelicci, T. Heinzel, Valproic acid defines a novel class of HDAC inhibitors inducing differentiation of transformed cells, EMBO J. 20 (2001) 6969–6978.
[9] A. Goyal, A. Srivastava, R. Sihota, J. Kaur, Evaluation of oxidative stress markers in aqueous humor of primary open angle glaucoma and primary angle closure glaucoma patients, Curr. Eye Res. 39 (2014) 823–829.
[10] N. Gurvich, P.S. Klein, Lithium and valproic acid: parallels and contrasts in diverse signaling contexts, Pharmacol. Ther. 96 (2002) 45–66.
[11] Y. Hao, T. Creson, L. Zhang, P. Li, F. Du, P. Yuan, T.D. Gould, H.K. Manji, G. Chen, Mood stabilizer valproate promotes ERK pathway-dependent cortical neuronal growth and neurogenesis, J. Neurosci. 24 (2004) 6590–6599.
[12] C. Harada, X. Guo, K. Namekata, A. Kimura, K. Nakamura, K. Tanaka, L.F. Parada, T. Harada, Glia- and neuron-specific functions of TrkB signalling during retinal degeneration and regeneration, Nat. Commun. 2 (2011) 189.
[13] C. Harada, T. Harada, Neurotrophic factors, in: T. Nakazawa, Y. Kitaoka, T. Harada (Eds.), Neuroprotection and Neuroregeneration for Retinal Diseases, Springer, Japan, 2014, pp. 99–112.
[14] C. Harada, K. Nakamura, K. Namekata, A. Okumura, Y. Mitamura, Y. Iizuka, K. Kashiwagi, K. Yoshida, S. Ohno, A. Matsuzawa, K. Tanaka, H. Ichijo, T. Harada, Role of apoptosis signal-regulating kinase 1 in stress-induced neural cell apoptosis in vivo, Am. J. Pathol. 168 (2006) 261–269.
[15] C. Harada, K. Namekata, X. Guo, H. Yoshida, Y. Mitamura, Y. Matsumoto, K. Tanaka, H. Ichijo, T. Harada, ASK1 deficiency attenuates neural cell death in GLAST-deficient mice, a model of normal tension glaucoma, Cell Death Differ. 17 (2010) 1751–1759.
[16] T. Harada, C. Harada, K. Nakamura, H.M. Quah, A. Okumura, K. Namekata, T. Saeki, M. Aihara, H. Yoshida, A. Mitani, K. Tanaka, The potential role of glutamate transporters in the pathogenesis of normal tension glaucoma, J. Clin. Invest. 117 (2007) 1763–1770.
[17] J. Hoffmann, S. Akerman, P.J. Goadsby, Efficacy and mechanism of anticonvulsant drugs in migraine, Expert Rev. Clin. Pharmacol. 7 (2014) 191–201.
[18] A. Iwase, Y. Suzuki, M. Araie, T. Yamamoto, H. Abe, S. Shirato, Y. Kuwayama, H.K. Mishima, H. Shimizu, G. Tomita, Y. Inoue, Y. Kitazawa, J.G.S. Tajimi Study Group, the prevalence of primary open-angle glaucoma in Japanese: the Tajimi Study, Ophthalmology 111 (2004) 1641–1648.
[19] U. Kilic, E. Kilic, A. Jarve, Z. Guo, A. Spudich, K. Bieber, U. Barzena, C.L. Bassetti, H.H. Marti, D.M. Hermann, Human vascular endothelial growth factor protects axotomized retinal ganglion cells in vivo by activating ERK-1/2 and Akt pathways, J. Neurosci. 26 (2006) 12439–12446.
[20] A. Kimura, K. Namekata, X.T. Guo Noro, C. Harada, T. Harada, Valproic acid prevents NMDA-induced retinal ganglion cell death via stimulation of neuronal TrkB receptor signaling, Am. J. Pathol. (2015), in press.
[21] W. Loscher, Basic pharmacology of valproate: a review after 35 years of clinical use for the treatment of epilepsy, CNS Drugs 16 (2002) 669–694.

[22] H.J. Majima, T. Nakanishi-Ueda, T. Ozawa, 4-Hydroxy-2-nonenal (4-HNE) staining by anti-HNE antibody, Methods Mol. Biol. 196 (2002) 31–34.
[23] M. Michaelis, T. Suhan, U.R. Michaelis, K. Beek, F. Rothweiler, L. Tausch, O. Werz, D. Eikel, M. Zornig, H. Nau, I. Fleming, H.W. Doerr, J. Cinatl Jr., Valproic acid induces extracellular signal-regulated kinase 1/2 activation and inhibits apoptosis in endothelial cells, Cell Death Differ. 13 (2006) 446–453.
[24] B. Monti, E. Polazzi, A. Contestabile, Biochemical, molecular and epigenetic mechanisms of valproic acid neuroprotection, Curr. Mol. Pharmacol. 2 (2009) 95–109.
[25] K. Namekata, C. Harada, X. Guo, K. Kikushima, A. Kimura, N. Fuse, Y. Mitamura, K. Kohyama, Y. Matsumoto, K. Tanaka, T. Harada, Interleukin-1 attenuates normal tension glaucoma-like retinal degeneration in EAAC1-deficient mice, Neurosci. Lett. 465 (2009) 160–164.
[26] K. Namekata, C. Harada, K. Kohyama, Y. Matsumoto, T. Harada, Interleukin-1 stimulates glutamate uptake in glial cells by accelerating membrane trafficking of Na^+/K^+-ATPase via actin depolymerization, Mol. Cell. Biol. 28 (2008) 3273–3280.
[27] K. Namekata, A. Kimura, K. Kawamura, X. Guo, C. Harada, K. Tanaka, T. Harada, Dock3 attenuates neural cell death due to NMDA neurotoxicity and oxidative stress in a mouse model of normal tension glaucoma, Cell Death Differ. 20 (2013) 1250–1256.
[28] K. Namekata, A. Kimura, K. Kawamura, C. Harada, T. Harada, Dock GEFs and their therapeutic potential: neuroprotection and axon regeneration, Prog. Retin. Eye Res. 43 (2014) 1–16.
[29] N.N. Osborne, S. del Olmo-Aguado, Maintenance of retinal ganglion cell mitochondrial functions as a neuroprotective strategy in glaucoma, Curr. Opin. Pharmacol. 13 (2013) 16–22.
[30] C.J. Phiel, F. Zhang, E.Y. Huang, M.G. Guenther, M.A. Lazar, P.S. Klein, Histone deacetylase is a direct target of valproic acid, a potent anticonvulsant, mood stabilizer, and teratogen, J. Biol. Chem. 276 (2001) 36734–36741.
[31] H.A. Quigley, A.T. Broman, The number of people with glaucoma worldwide in 2010 and 2020, Br. J. Ophthalmol. 90 (2006) 262–267.
[32] R. Roskoski Jr., ERK1/2 MAP kinases: structure, function, and regulation, Pharmacol. Res. 66 (2012) 105–143.
[33] K. Semba, K. Namekata, X. Guo, C. Harada, T. Harada, Y. Mitamura, Renin-angiotensin system regulates neurodegeneration in a mouse model of normal tension glaucoma, Cell Death Dis. 5 (2014) e1333.
[34] K. Semba, K. Namekata, A. Kimura, C. Harada, Y. Mitamura, T. Harda, Brimonidine prevents neurodegeneration in a mouse model of normal tension glaucoma, Cell Death Dis. 5 (2014) e1341.
[35] D.I. Sinn, S.J. Kim, K. Chu, K.H. Jung, S.T. Lee, E.C. Song, J.M. Kim, D.K. Park, S. Kun Lee, M. Kim, J.K. Roh, Valproic acid-mediated neuroprotection in intracerebral hemorrhage via histone deacetylase inhibition and transcriptional activation, Neurobiol. Dis. 26 (2007) 464–472.
[36] S. Suda, K. Katsura, T. Kanamaru, M. Saito, Y. Katayama, Valproic acid attenuates ischemia-reperfusion injury in the rat brain through inhibition of oxidative stress and inflammation, Eur. J. Pharmacol. 707 (2013) 26–31.
[37] A.M. Waszkielewicz, A. Gunia, K. Sloczynska, H. Marona, Evaluation of anticonvulsants for possible use in neuropathic pain, Curr. Med. Chem. 18 (2011) 4344–4358.
[38] M.L. Zeise, S. Kasparow, W. Zieglgansberger, Valproate suppresses *N*-methyl-D-aspartate-evoked, transient depolarizations in the rat neocortex in vitro, Brain Res. 544 (1991) 345–348.
[39] C. Zhang, J. Zhu, J. Zhang, H. Li, Z. Zhao, Y. Liao, X. Wang, J. Su, S. Sang, X. Yuan, Q. Liu, Neuroprotective and anti-apoptotic effects of valproic acid on adult rat cerebral cortex through ERK and Akt signaling pathway at acute phase of traumatic brain injury, Brain Res. 1555 (2014) 1–9.
[40] Z. Zhang, X. Qin, N. Tong, X. Zhao, Y. Gong, Y. Shi, X. Wu, Valproic acid-mediated neuroprotection in retinal ischemia injury via histone deacetylase inhibition and transcriptional activation, Exp. Eye Res. 94 (2012) 98–108.
[41] Z. Zhang, X. Qin, X. Zhao, N. Tong, Y. Gong, W. Zhang, X. Wu, Valproic acid regulates antioxidant enzymes and prevents ischemia/reperfusion injury in the rat retina, Curr. Eye Res. 37 (2012) 429–437.
[42] Z. Zhang, N. Tong, Y. Gong, Q. Qiu, L. Yin, X. Lv, X. Wu, Valproate protects the retina from endoplasmic reticulum stress-induced apoptosis after ischemia-reperfusion injury, Neurosci. Lett. 504 (2011) 88–92.
[43] Z.Z. Zhang, Y.Y. Gong, Y.H. Shi, W. Zhang, X.H. Qin, X.W. Wu, Valproate promotes survival of retinal ganglion cells in a rat model of optic nerve crush, Neuroscience 224 (2012) 282–293.
[44] Y. Zhou, V. Pernet, W.W. Hauswirth, A. Di Polo, Activation of the extracellular signal-regulated kinase 1/2 pathway by AAV gene transfer protects retinal ganglion cells in glaucoma, Mol. Ther. 12 (2005) 402–412.

The 5-Year Incidence of Bleb-Related Infection and Its Risk Factors after Filtering Surgeries with Adjunctive Mitomycin C

Collaborative Bleb-Related Infection Incidence and Treatment Study 2

*Tetsuya Yamamoto, MD, PhD,[1] Akira Sawada, MD, PhD,[1] Chihiro Mayama, MD, PhD,[2] Makoto Araie, MD, PhD,[2] Shinji Ohkubo, MD, PhD,[3] Kazuhisa Sugiyama, MD, PhD,[3] Yasuaki Kuwayama, MD, PhD,[4] on behalf of The Collaborative Bleb-Related Infection Incidence and Treatment Study Group**

Purpose: To report the 5-year incidence of bleb-related infection after mitomycin C–augmented glaucoma filtering surgery and to investigate the risk factors for infections.

Design: Prospective, observational cohort study.

Participants: A total of 1098 eyes of 1098 glaucoma patients who had undergone mitomycin C–augmented trabeculectomy or trabeculectomy combined with phacoemulsification and intraocular lens implantation performed at 34 clinical centers.

Methods: Patients were followed up at 6-month intervals for 5 years, with special attention given to bleb-related infections. The follow-up data were analyzed via Kaplan-Meier survival analysis and the Cox proportional hazards model.

Main Outcome Measures: Incidence of bleb-related infection over 5 years and risk factors for infections.

Results: Of the 1098 eyes, a bleb-related infection developed in 21 eyes. Kaplan-Meier survival analysis revealed that the incidence of bleb-related infection was 2.2±0.5% (cumulative incidence ± standard error) at the 5-year follow-up for all cases, whereas it was 7.9±3.1% and 1.7±0.4% for cases with and without a history of bleb leakage, respectively ($P = 0.000$, log-rank test). When only eyes with a well-functioning bleb were counted, it was 3.9±1.0%. No differences were found between the trabeculectomy cases and the combined surgery cases ($P = 0.398$, log-rank test) or between cases with a fornix-based flap and those with a limbal-based flap ($P = 0.651$, log-rank test). The Cox model revealed that a history of bleb leakage and younger age were risk factors for infections.

Conclusions: The 5-year cumulative incidence of bleb-related infection was 2.2±0.5% in eyes treated with mitomycin C–augmented trabeculectomy or trabeculectomy combined with phacoemulsification and intraocular lens implantation in our prospective, multicenter study. Bleb leakage and younger age were the main risk factors for infections. *Ophthalmology 2014;121:1001-1006 © 2014 by the American Academy of Ophthalmology.*

**Supplemental material is available at www.aaojournal.org.*

Mitomycin C (MMC), an antitumor antibiotic, improves intraocular pressure control after glaucoma filtering surgery when used during surgery as an adjunctive therapy.[1] This favorable effect is brought about by inhibited proliferation of Tenon's fibroblasts.[2] Glaucoma surgery using antiproliferative agents, however, increases the incidence of some postoperative complications,[3,4] including bleb-related infection, which is a potentially blinding condition. The proportion of patients in whom the postinfection visual acuity was 20/400 or better was reported to be 22% to 57% in bleb-related endophthalmitis.[5–9] In our series consisting of cases in which visual acuity was at least 20/40 before infection, the incidence of cases in which the ratio of postinfection visual acuity was 20/400 or better was 56% in bleb-related infections with vitreous involvement.[10]

We initiated the Collaborative Bleb-Related Infection Incidence and Treatment Study[11] (CBIITS), a 5-year prospective study, to investigate the incidence, severity, and prognosis of bleb-related infection and to explore the efficacy of a predetermined antibacterial management strategy for these infections. Our interim report[11] documented a cumulative incidence of bleb-related infection of 1.5±0.6% (cumulative incidence ± standard error [SE]) at the 2.5-year follow-up in eyes that underwent MMC-augmented trabeculectomy or trabeculectomy combined with phacoemulsification and

ISSN 0161-6420/14/$ - see front matter
http://dx.doi.org/10.1016/j.ophtha.2013.11.025

intraocular lens implantation. This article describes the final 5-year clinical data on the incidence of and risk factors for bleb-related infection after filtering surgery with adjunctive MMC.

Methods

The CBIITS is a multicenter, prospective cohort study with the primary outcome measure being the incidence of and risk factors for bleb-related infection. The efficacy of the predetermined treatment protocol in this study also was investigated in a prospective fashion. The details of the CBIITS are described elsewhere.[11] In brief, the enrollment period was 2 years and follow-up was carried out every 6 months for up to 5 years. Ophthalmologic examinations were conducted at each follow-up according to the protocol. Surgical technique and postoperative management were at the discretion of local investigators. If bleb-related infection was noted, additional examinations were conducted and the predetermined treatment was initiated rapidly, depending on the stage of the infection. Thirty-four institutions participated in the CBIITS. The clinical centers and a list of investigators are shown in Appendix 1 (available at www.aaojournal.org). Institutional review board approval was obtained at each institution and all patients gave written informed consent after a thorough explanation of the study. In the CBIITS, bleb-related infection was defined as an infection fulfilling all of the following 3 conditions: (1) history of filtering surgery, (2) an episode developed no sooner than 4 weeks after surgery, and (3) clinical signs of infection related to a filtering bleb microscopically confirmed by slit lamp. Infection was classified into the following 3 stages: stage I or blebitis denotes infections confined to the bleb site with a mild cell reaction in the anterior chamber, stage II denotes infections wherein the anterior chamber is the main locus and the vitreous is not involved, and stage III denotes infections involving the posterior part of the eye.[11–13] Stage III is subdivided further into stages IIIa and IIIb, as follows: stage IIIa denotes mild involvement of the vitreous and stage IIIb denotes more advanced involvement.

In this report, we discuss the incidence of bleb-related infection and risk factors for infection in MMC-augmented cases, in total and in some subgroups for which follow-up data were available for at least 1 year after surgery. Kaplan-Meier survival analysis and the Cox proportional hazards model were applied. The analysis was conducted via SPSS software version 20.0 (IBM Japan Ltd., Tokyo, Japan).

As previously reported,[11] the CBIITS enrolled 1249 eyes of 1249 patients. The present study included 1098 eyes of 1098 patients who were treated with trabeculectomy or with combined surgery with MMC. A total of 151 eyes were excluded from the 1249 subjects in the present study for the following reasons: 38 eyes had been treated with surgical techniques other than trabeculectomy alone or trabeculectomy combined with phacoemulsification and intraocular lens implantation, 65 eyes had undergone surgery without adjunctive MMC, and 48 cases were lost to follow-up before the 1-year follow-up (Fig 1).

A total of 824 eyes (75.0%) completed the 5-year follow-up or reached the end point, that is, the development of infection. The remaining 274 eyes (25.0%) were lost to follow-up after reaching 1 year. The reasons for the loss of follow-up after reaching 1 year were moving location in 14 patients (1.3%), death of 38 patients (3.5%), health problems unrelated to ocular diseases in 43 patients (3.9%), change of hospitals in 92 patients (8.4%), and undetermined in the remaining 87 patients (7.9%; Fig 1). Table 1 (available at www.aaojournal.org) shows the comparison of uninfected patients who completed the 5-year follow-up and those who did not. The follow-up period averaged 51.9±15.5 months (mean ± standard deviation [SD]) and ranged from 12 to 60 months. The types of filtering surgeries were trabeculectomy in 916 eyes and trabeculectomy with phacoemulsification and intraocular lens implantation in 182 eyes. A fornix-based conjunctival flap was prepared in 473 eyes (358 eyes in the trabeculectomy group and 115 eyes and the combined surgery group); a limbal-based conjunctival flap was prepared in 625 eyes (558 eyes in the trabeculectomy group and 67 eyes and the combined surgery group). During the 5-year follow-up, the following additional glaucoma surgeries were conducted in a total of 57 eyes: trabeculectomy in 46 eyes, nonpenetrating trabeculectomy in 1 eye, trabeculectomy combined with phacoemulsification and intraocular lens implantation in 3 eyes, implantation of glaucoma drainage devices in 2 eyes, and cyclophotocoagulation in 5 eyes. The age averaged 63.7±13.1 years (mean ± SD) and ranged from 13 to 92 years at the time of surgery. The surgery was the first glaucoma surgery in 882 eyes. A total of 151 eyes had a history of 1 previous glaucoma surgery, and the remaining 65 eyes had undergone at least 2 previous glaucoma surgeries. Six hundred forty-eight patients were men and 450 patients were women. Five hundred

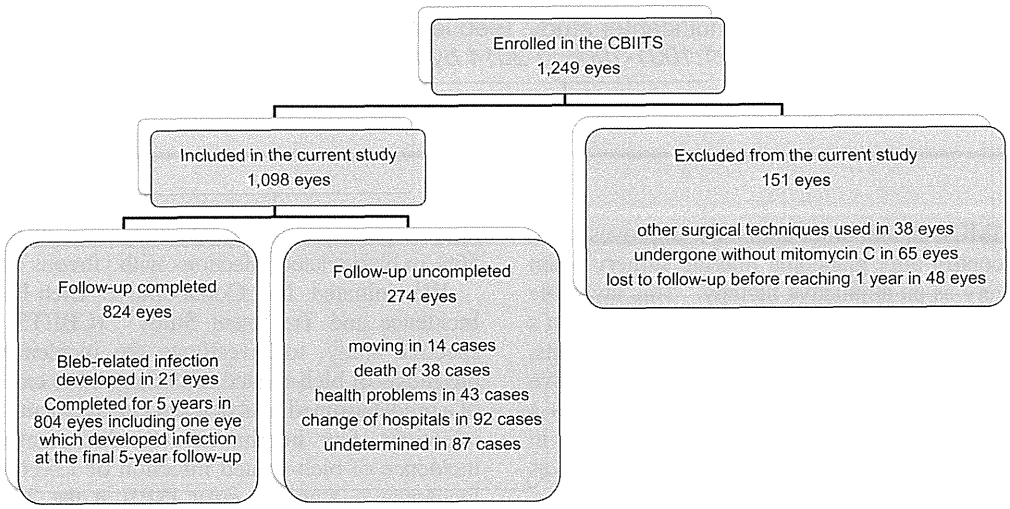

Figure 1. Flow chart showing the number of patients enrolled and analyzed. CBIITS = Collaborative Bleb-Related Infection Incidence and Treatment Study.

fifty-eight eyes were right eyes and 540 eyes were left eyes. The method of MMC application varied among surgeons: the concentration ranged between 0.2 and 0.5 mg/ml and the duration of application ranged between 2 and 5 minutes. Thirty eyes received subconjunctival injections of 5-fluorouracil after surgery in addition to intraoperative MMC. The types of glaucoma were primary open-angle glaucoma in 485 eyes (44.2%), juvenile-onset glaucoma in 26 eyes (2.4%), normal-tension glaucoma in 68 eyes (6.2%), primary angle-closure glaucoma in 68 eyes (6.2%), mixed primary open-angle glaucoma and primary angle-closure glaucoma in 2 eyes (0.2%), and secondary glaucoma in 449 eyes (40.9%). The diagnosis of secondary glaucoma were exfoliative glaucoma in 120 eyes, glaucoma secondary to uveitis in 116 eyes, neovascular glaucoma in 96 eyes, glaucoma related to intraocular surgery in 29 eyes, posttraumatic glaucoma in 17 eyes, other types of secondary glaucoma in 34 eyes, and unidentified in the remaining 37 eyes. Eighty-three eyes were rated with positive conjunctival leakage during the 5-year follow-up because Seidel testing results were positive at least once.

Results

Bleb-related infection developed in 21 eyes during the entire follow-up period. One eye of the 21 showed a repeated episode of infection. The stage of bleb-related infection at diagnosis was stage I in 10 eyes (47.6%), stage II in 6 eyes (28.6%), stage IIIa in 2 eyes (9.5%), and stage IIIb in 3 eyes (14.3%). A diagnosis of bleb-related infection was made in 1 patient while she was on a trip to the Unites States. She was treated with topical tobramycin eyedrops and completely recovered to her preinfection status without any sequelae 1 month later when she sought a consultation with a study investigator. Based on her mild clinical course, the case was regarded as a stage I infection for the purposes of this study. The period between glaucoma surgery and the onset of infection was 27.3±15.9 months (mean ± SD) and ranged from 3 to 60 months. Eight infections developed in eyes with a fornix-based flap and 13 infections developed in eyes with a limbal-based flap. The type of filtering surgeries in the infection cases were 19 eyes after trabeculectomy and 2 eyes after combined surgery. Six eyes were found to have bleb leakage before the infection, which developed 4 to 27 months (mean ± SD, 17.0±8.5 months) after the first leakage was noted. Bleb leakage was noted in 1 eye when infection was diagnosed. Eight eyes were receiving topical antibiotic therapy at the time of infection.

Kaplan-Meier survival analysis revealed that the incidence of development of bleb-related infection was 2.2±0.5% (calculated cumulative incidence ± SE) at the 5-year follow-up (Fig 2). The incidence was 1.9±0.7% (cumulative incidence ± SE) and 2.3±0.6% at the 5-year follow-up in cases with a fornix-based flap and those with a limbal-based flap, respectively ($P = 0.651$, log-rank test; Fig 3). When subdivided into the trabeculectomy group and the combined surgery group, the incidence was 2.4±0.5% (cumulative incidence ± SE) and 1.1±0.8%, respectively, at the 5-year follow-up ($P = 0.398$, log-rank test; Fig 4). When cases with a history of bleb leakage were compared with those without leakage, the incidence was 7.9±3.1% (cumulative incidence ± SE) and 1.7±0.4%, respectively, at the 5-year follow-up (Fig 5), and the difference was significant ($P = 0.000$, log-rank test).

When only patients who completed the 5-year follow-up or in whom infection developed were taken into account, the incidence of bleb-related infection was 2.5% in all patients, 2.4% in those with a fornix-based flap, 2.8% in those with a limbal-based flap, 2.8% in the trabeculectomy group, 1.6% in the combined surgery group, 10.3% in those with a history of bleb leakage, and 2.0% in those without leakage.

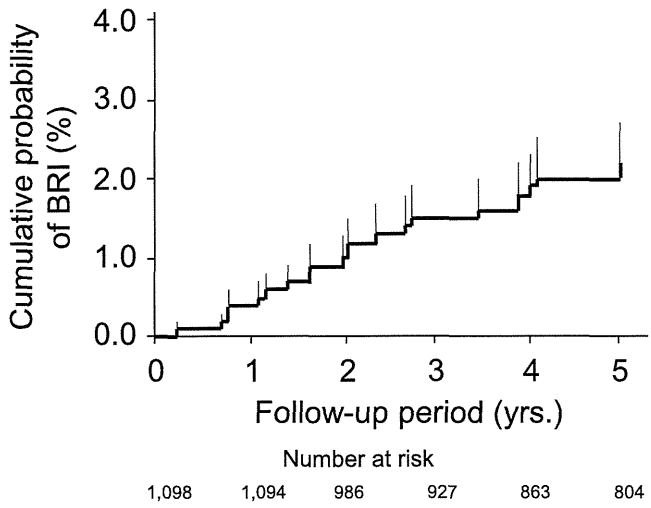

Figure 2. Kaplan-Meier estimates for the incidence of a bleb-related infection (BRI) developing after filtering surgeries with mitomycin C in 1098 eyes. The incidence was 2.2±0.5% at the 5-year follow-up (cumulative incidence ± standard error). Fine lines denote standard errors.

In all cases with endophthalmitis, that is, stage II and stage III disease, the incidence was 1.1±0.3%; the incidence was 1.0±0.5% and 1.2±0.5% (cumulative incidence ± SE) at the 5-year follow-up for cases with a fornix-based flap and those with a limbal-based flap, respectively (Figs 6 and 7, available at www.aaojournal.org). There were no significant differences in the incidence of development of infection between the 2 groups ($P = 0.656$, log-rank test). The incidence of bleb-related infection was 1.4% in patients with endophthalmitis when only patients who completed the 5-year follow-up or in whom infection developed were taken into account.

During the postoperative period in which a well-functioning bleb was considered to be present, the incidence increased to 3.9±1.0% for all patients; it was 3.9±1.5% and 4.0±1.3%

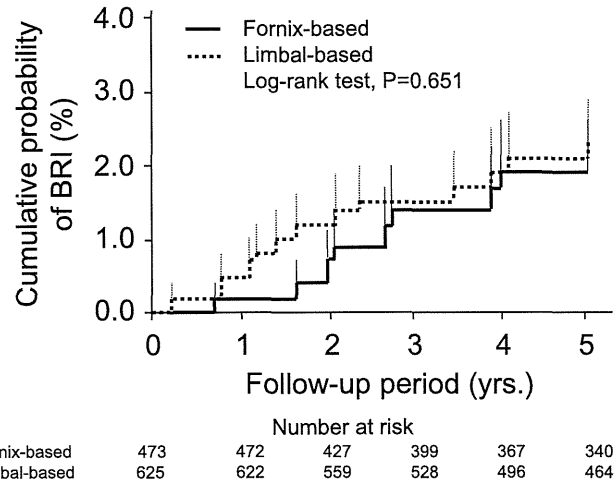

Figure 3. Kaplan-Meier estimates for the incidence of a bleb-related infection (BRI) developing after filtering surgeries with mitomycin C in 473 eyes with a fornix-based conjunctival flap and 625 eyes with a limbal-based flap. The incidence was 1.9±0.7% and 2.3±0.6% at the 5-year follow-up (cumulative incidence ± standard error) for fornix-based and limbal-based flaps, respectively. Fine lines denote standard errors.

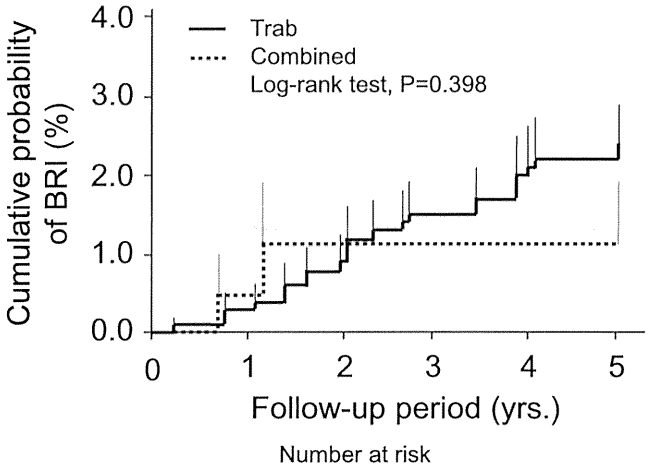

Number at risk

Trab	916	913	822	775	727	677
Combined	182	181	164	152	136	127

Figure 4. Kaplan-Meier estimates for the incidence of a bleb-related infection (BRI) developing after filtering surgeries with mitomycin C in 916 eyes that underwent trabeculectomy (Trab) and 182 eyes that underwent trabeculectomy with phacoemulsification and intraocular lens implantation (Combined). The incidence was 2.4±0.5% and 1.1±0.8% at the 5-year follow-up (cumulative incidence ± standard error) for trabeculectomy and trabeculectomy with phacoemulsification and intraocular lens implantation, respectively. Fine lines denote standard errors.

(cumulative incidence ± SE) at the 5-year follow-up for patients with a fornix-based flap and those with a limbal-based flap, respectively (Fig 8). No significant differences were found between the 2 groups ($P = 0.984$, log-rank test). In the last analysis, an eye with a well-functioning bleb was defined as one having intraocular pressure within 15 mmHg, without any antiglaucoma medications except oral carbonic anhydrase inhibitors for the fellow eye,

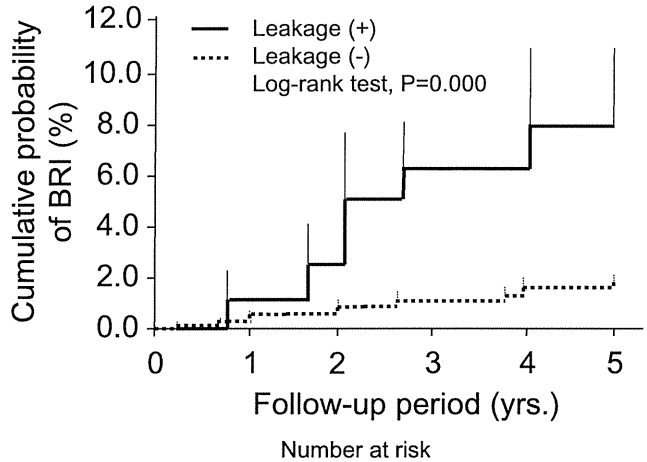

Number at risk

Leakage (+)	83	82	78	70	65	58
Leakage (-)	1,015	1,012	908	857	798	746

Figure 5. Kaplan-Meier estimates for the incidence of a bleb-related infection (BRI) developing after filtering surgeries with mitomycin C in 83 eyes with postoperative conjunctival leakage during the follow-up period and 1015 eyes without leakage. The incidence was 7.9±3.1% and 1.7±0.4% at the 5-year follow-up (cumulative incidence ± standard error) for cases with leakage and those without leakage, respectively. Fine lines denote standard errors.

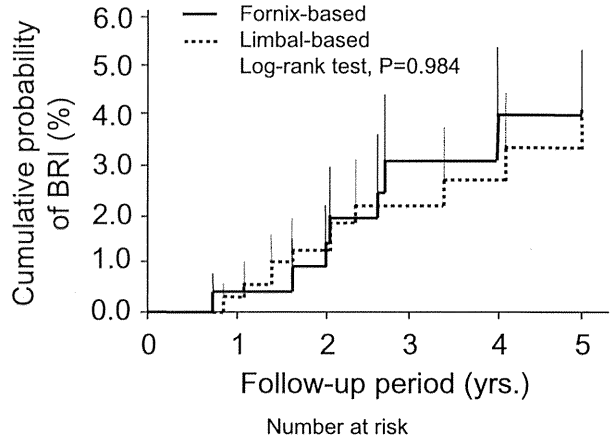

Number at risk

Fornix-based	473	269	200	159	131	114
Limbal-based	625	352	258	205	173	149

Figure 8. Kaplan-Meier estimates for the incidence of a bleb-related infection (BRI) developing in cases with a well-functioning bleb after filtering surgeries with mitomycin C in 473 eyes with a fornix-based conjunctival flap and 625 eyes with a limbal-based flap. The incidence was 3.9±1.5% and 4.0±1.3% at the 5-year follow-up (cumulative incidence ± standard error) for fornix-based and limbal-based flaps, respectively. Fine lines denote standard errors. Refer to the text for the definition of a well-functioning bleb.

without any additional glaucoma surgery except bleb revision, and having a bleb larger than the size of the scleral flap. Using this definition, 5 of the 21 infections were not counted as infections when the Kaplan-Meier analysis was applied to this subgroup because the infection developed after the eye failed to meet the criteria for a functioning bleb. Of the 5 eyes, 4 eyes had a small but partly avascular bleb and the remaining 1 eye had a totally vascularized bleb. The stage of bleb-related infection was stage I in 9 eyes, stage II in 4 eyes, stage IIIa in 1 eye, and stage IIIb in 2 eyes in the well-functioning blebs.

The Cox proportional hazards model found that a positive history of bleb leakage during the follow-up and younger age were significant risk factors for the development of bleb-related infection (Table 2). Factors that were not significant included the type of surgery (trabeculectomy alone or combined), the type of conjunctival incision (fornix-based or limbal-based), laterality, sex, and the presence of a well-functioning bleb during the entire follow-up period.

Visual acuity did not change by more than 2 lines in stage I infections when the acuity before infection was compared with that at 6 months after infection, whereas it deteriorated by more than 2 lines in 1 eye with stage II infection and in 3 eyes with stage III infection.

Discussion

Although a functioning filtering bleb is the basis for a successful filtering surgery, a filtering bleb can cause significant late-onset complications in some cases.[3,4] In fact, bleb-related infection is a major late-onset complication of these surgeries. This study found that a bleb-related infection developed with an incidence of 2.2±0.5% (cumulative incidence ± SE) at the 5-year follow-up in patients who underwent trabeculectomy or trabeculectomy combined with phacoemulsification and intraocular lens implantation with adjunctive **MMC** in a prospective fashion. When only

Table 2. Results of the Cox Proportional Hazards Model for Risk Factors of Bleb-Related Infections

Variable	Value	Odds Ratio	95% Confidence Interval	*P* Value
Bleb leakage	Yes	4.710	1.827–12.142	0.001
	No	1		
Age		0.719 per 10 years older	0.536–0.965	0.024

Factors not significantly associated: type of surgery, type of conjunctival incision, laterality, sex, and presence of well-functioning bleb during the entire follow-up period, as defined in the text.

apparently well-functioning blebs were counted, it was estimated to be 3.9±1.0%. Of the 5 eyes that failed to meet the criteria for a functioning bleb, but in which bleb-related infection developed, 4 eyes had a small but partly avascular bleb. This result suggests that bleb-related infection is related at least partly to the existence of a thin and avascular bleb. Several previous studies have reported the incidence of bleb-related infection in a prospective manner. For example, Zahid et al[14] reported a 5-year incidence of blebitis and endophthalmitis of 1.5% and 1.1%, respectively, in the Collaborative Initial Glaucoma Treatment Study of 285 patients, including 163 patients (57%) in whom 5-fluorouracil was used adjunctively with trabeculectomy. Gedde et al[15] also reported that 4.8% of 105 eyes demonstrated bleb-related infection after trabeculectomy in the Tube Versus Trabeculectomy Study. Additionally, Solus et al[3] estimated a 1.2% per year rate of late infections for limbus-based surgery and a 0.3% per year rate for fornix-based surgery for the first 4 years after surgery in a retrospective study. The present study is unique in paying special attention to bleb-related infection and in focusing on its incidence in a prospective fashion. It is also unique for its large sample size, with the number of eyes followed up exceeding 1000. Despite the uniform Japanese ethnicity of our patient population, these findings provide useful guidelines and source data for the consideration of different surgical approaches and possible outcomes. We will present detailed data on the effect of our predetermined management strategy for bleb-related infection in the future.

Several factors are known to be associated significantly with the development of bleb-related infection, with the major factors including the use of antiproliferatives,[16] an inferiorly located bleb,[17] the presence of bleb leakage,[17–19] and the use of a limbal-based conjunctival flap.[20] In the present analysis, all cases were treated adjunctively with MMC and all but 12 eyes (1.1%), including 8 in which the 3- or 9-o'clock positions were used, underwent a surgery in the superior half of the limbal circumference. Thus, we were unable to evaluate the relative risk of MMC or the location of the bleb against the development of bleb-related infection. Bleb leakage again was found to be the greatest risk factor in this study. A positive history of bleb leakage was associated with a 4.71-fold increase in the risk of infection. Consistent with previous studies,[17–19] our findings suggest that bleb leakage should be repaired or treated appropriately as soon as it is noted.

According to Wells et al,[20] a limbus-based conjunctival flap causes more serious complications, including bleb-related infection, in pediatric and young adult eyes compared with a fornix-based flap. Solus et al[3] reported that bleb-related infection was more common in eyes with a limbus-based flap than in those with a fornix-based flap and that the hazard ratio was 3.39 ($P = 0.054$; 17 with a fornix-based flap and 20 with a limbus-based flap) based on the Cox proportional hazard analysis. Solus et al also noted that late infections occurred significantly later in limbus-based conjunctival flaps. In contrast to these earlier studies,[3,20] we found no significant differences in outcomes between the fornix-based conjunctival flap and the limbal-based flap in the total patients or in those with a well-functioning bleb. Similarly, we found no significant difference in the time to development of bleb-related infection in fornix- or limbal-based flaps. The reason for the discrepancy between this and previous reports[3,20] is unknown, but we speculate that the morphologic feature of the filtering bleb in Japanese patients may differ from that of other ethnic groups.

The present findings also revealed that younger age was a risk factor. Likewise, Wolner et al[21] reported that late-onset bleb-related endophthalmitis was more common in patients younger than 60 years after trabeculectomy with adjunctive 5-fluorouracil. However, Higginbotham et al[22] and Greenfield et al[23] did not find an age-related influence in patients treated with adjunctive MMC. In any case, it is possible that age-related differences in levels of physical activity could influence the development of infection by affecting the level of exposure to infective agents or trauma to the bleb.

Our study has several limitations. First, all surgeries were performed in Japan, across 34 centers, and this geographic and ethnic homogeneity could limit the applicability of the findings to clinical settings outside Japan. Second, because many different glaucoma specialists performed the follow-up examinations, interobserver differences might have affected the results, although our predetermined follow-up protocol might have minimized this effect. Third, the surgical technique was not identical among the centers or surgeons because the indication for surgery and the selection of the operative procedure were at the discretion of each investigator. The main purpose of this study, however, was to determine whether a formed filtering bleb represents a risk of infection, and so the effect of technical differences among surgeons was a minor consideration. Fourth, it is possible that a bleb-related infection was missed during the follow-up. To minimize this effect, we encouraged the patients to report immediately to the clinic if they noted any abnormal sensation or event, such as pain, redness, or discharge.

In summary, the incidence of bleb-related infection was estimated to be 2.2±0.5% (cumulative incidence ± SE) at the 5-year, prospective follow-up in 1098 eyes that underwent trabeculectomy or trabeculectomy combined with phacoemulsification and intraocular lens implantation with adjunctive MMC. The incidence was 3.9±1.0% when only apparently well-functioning blebs were counted. A history of bleb leakage and younger age were found to be risk

factors for infections. These results indicate the need for closer follow-up or treatment of patients with bleb leaks, selection of nonbleb procedures for younger patients whenever possible, and proper informed consent for any patients undergoing trabeculectomy to ensure better visual prognosis of glaucoma patients.

References

1. Kitazawa Y, Kawase K, Matsushita H, Minobe M. Trabeculectomy with mitomycin: a comparative study with fluorouracil. Arch Ophthalmol 1991;109:1693–8.
2. Yamamoto T, Varani J, Soong HK, Lichter PR. Effects of 5-fluorouracil and mitomycin C on cultured rabbit subconjunctival fibroblasts. Ophthalmology 1990;97:1204–10.
3. Solus JF, Jampel HD, Tracey PA, et al. Comparison of limbus-based and fornix-based trabeculectomy: success, bleb-related complications, and bleb morphology. Ophthalmology 2012;119:703–11.
4. Jampel HD, Solus JF, Tracey PA, et al. Outcomes and bleb-related complications of trabeculectomy. Ophthalmology 2012;119:712–22.
5. Song A, Scott IU, Flynn HW, Budenz DL. Delayed-onset bleb-associated endophthalmitis: clinical features and visual acuity outcomes. Ophthalmology 2002;109:985–91.
6. Kangas TA, Greenfield DS, Flynn HW Jr, et al. Delayed-onset endophthalmitis associated with conjunctival filtering blebs. Ophthalmology 1997;104:746–52.
7. Ciulla TA, Beck AD, Topping TM, Baker AS. Blebitis, early endophthalmitis and late endophthalmitis after glaucoma-filtering surgery. Ophthalmology 1997;104:986–95.
8. Mandelbaum S, Forster RK, Gelender H, Culbertson W. Late onset endophthalmitis associated with filtering blebs. Ophthalmology 1985;92:964–72.
9. Leng T, Miller D, Flynn HW Jr, et al. Delayed-onset bleb-associated endophthalmitis (1996–2008): causative organisms and visual acuity outcomes. Retina 2011;31:344–52.
10. Yamamoto T, Kuwayama Y, Nomura E, et al; Study Group for the Japan Glaucoma Society Survey of Bleb-Related Infection. Changes in visual acuity and intra-ocular pressure following bleb-related infection: the Japan Glaucoma Society Survey of Bleb-related Infection Report 2 [report online]. Acta Ophthalmol 2013;91:e420–6.
11. Yamamoto T, Kuwayama Y; Collaborative Bleb-Related Infection Incidence and Treatment Study Group. Interim clinical outcomes in the Collaborative Bleb-Related Infection Incidence and Treatment Study. Ophthalmology 2011;118:453–8.
12. Azuara-Branco A, Katz LJ. Dysfunctional filtering blebs. Surv Ophthalmol 1998;43:93–126.
13. Greenfield DS. Bleb-related ocular infection. J Glaucoma 1998;7:132–6.
14. Zahid S, Musch DC, Niziol LM, et al; Collaborative Initial Glaucoma Treatment Study Group. Risk of endophthalmitis and other long-term complications of trabeculectomy in the Collaborative Initial Glaucoma Treatment Study (CIGTS). Am J Ophthalmol 2013;155:674–80.
15. Gedde SJ, Herndon LW, Brandt JD, et al; Tube Versus Trabeculectomy Study Group. Postoperative complications in the Tube Versus Trabeculectomy (TVT) study during five years of follow-up. Am J Ophthalmol 2012;153:804–14.
16. Jampel H, Quigley HA, Kerrigan-Baumrind LA, et al; Glaucoma Surgical Outcomes Study Group. Risk factors for late-onset infection following glaucoma filtration surgery. Arch Ophthalmol 2001;119:1001–8.
17. Soltau JB, Rothman RF, Budenz DL, et al. Risk factors for glaucoma filtering bleb infections. Arch Ophthalmol 2000;118:338–42.
18. Matsuo H, Tomidokoro A, Suzuki Y, et al. Late-onset trans-conjunctival oozing and point leak of aqueous humor from filtering bleb after trabeculectomy. Am J Ophthalmol 2002;133:456–62.
19. Yamamoto T, Kuwayama Y, Kano K, et al; Study Group for the Japan Glaucoma Society Survey of Bleb-Related Infection. Clinical features of bleb-related infection: a 5-year survey in Japan. Acta Ophthalmol 2013;91:619–24.
20. Wells AP, Cordeiro MF, Bunce C, Khaw PT. Cystic bleb formation and related complications in limbus- versus fornix-based conjunctival flaps in pediatric and young adult trabeculectomy with mitomycin C. Ophthalmology 2003;110:2192–7.
21. Wolner B, Liebmann JM, Sassani JW, et al. Late bleb-related endophthalmitis after trabeculectomy with adjunctive 5-fluorouracil. Ophthalmology 1991;98:1053–60.
22. Higginbotham EJ, Stevens RK, Musch DC, et al. Bleb-related endophthalmitis after trabeculectomy with mitomycin C. Ophthalmology 1996;103:650–6.
23. Greenfield DS, Suñer IJ, Miller MP, et al. Endophthalmitis after filtering surgery with mitomycin. Arch Ophthalmol 1996;114:943–9.

Footnotes and Financial Disclosures

Originally received: August 6, 2013.
Final revision: November 11, 2013.
Accepted: November 12, 2013.
Available online: January 13, 2014. Manuscript no. 2013-1306.

[1] Department of Ophthalmology, Gifu University Graduate School of Medicine, Gifu, Japan.

[2] Department of Ophthalmology, The University of Tokyo Graduate School of Medicine, Tokyo, Japan.

[3] Department of Ophthalmology and Visual Science, Kanazawa University Graduate School of Medical Science, Kanazawa, Japan.

[4] Department of Ophthalmology, Osaka Koseinenkin Hospital, Osaka, Japan.

*The clinical centers and investigators are listed in Appendix 1 (available at www.aaojournal.org).

Financial Disclosure(s):
The author(s) have no proprietary or commercial interest in any materials discussed in this article.

Correspondence:
Tetsuya Yamamoto, MD, PhD, Department of Ophthalmology, Gifu University Graduate School of Medicine, 1-1 Yanagido, Gifu-shi, Japan, 501-1194. E-mail: mmc-gif@umin.net.

6

I 緑内障診療の基本

緑内障に関連する遺伝子

ゲノムと遺伝子（図1）

- 「ゲノム（genome）」は「遺伝子（gene）の総体（-ome）」という意味を込めて作られた造語であるが，実際のゲノムは遺伝子だけでなく他のさまざまな塩基配列によって構成されている。
- 「ゲノム」は「遺伝子」とその他の領域（遺伝子砂漠領域：繰り返し配列，調節配列，非コードRNAをコードする配列など）すべてを含み，体細胞では約66億塩基対が24種類の染色体に分配されて核内に収納されている。
- 蛋白質をコードする遺伝子はプロモーター，エキソン，イントロン，5′UTR（untranslated region），3′UTRの4つの領域から構成され，ゲノム全体のわずか2%に過ぎない。
- ヒト同士のゲノム配列の相同性は約99～99.5%であり，ヒトの個人差を規定する配列の違い（バリアントと総称する）は約0.5～1%で，数千万塩基対に相当する。

1000Kアレイ（図2）

- DNAマイクロアレイ（アレイやチップと呼称される）は，アフィメトリクス製とイルミナ製のものが主流である。
- アフィメトリクスの1000Kアレイでは，ゲノム上に存在する約100万個の一塩基多型［single nucleotide polymorphism（SNP）：集団におけるアレル頻度が1%以上のバリアントを特にSNPとよぶ］を調べることができる。
- 1000Kアレイでは500ngのゲノムDNAを出発材料とし，3日間のプロトコールでデータを取得する。アレイ上のプローブと断片化したゲノムDNAとのハイブリダイゼーションの有無を専用スキャナで読み取り，SNPを決定（ジェノタイピング）する。
- アレイ上のSNPを検出するためのプローブは白人に最適化され，日本人では約40%がSNPではなく，実際には約60%しか解析に使用できない。

図1　ゲノムと遺伝子

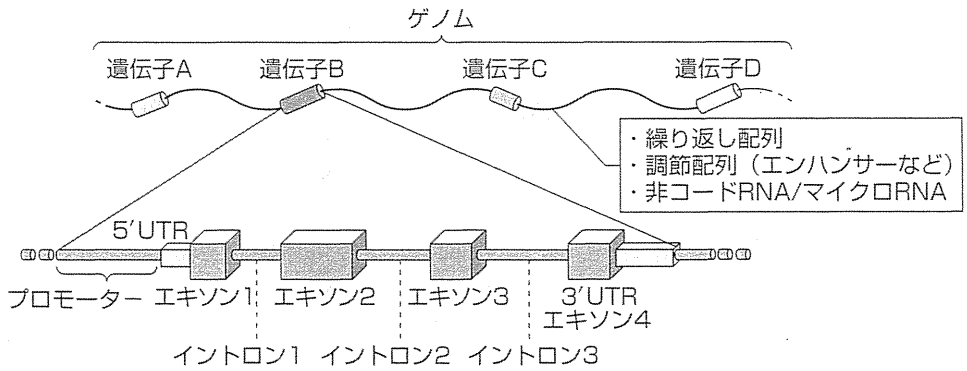

図2　1000Kアレイ